NASA TECHNICAL NOTE

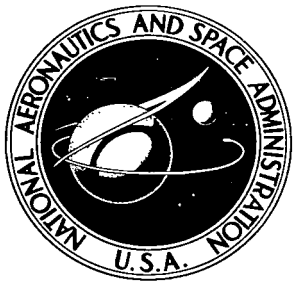

NASA TN D-8415

C.1

NASA TN D-8415

LOAN COPY: RETURN
AFWL TECHNICAL LIBR
KIRTLAND AFB, N. M

AEROTHERMAL AND STRUCTURAL PERFORMANCE OF A COBALT-BASE SUPERALLOY THERMAL PROTECTION SYSTEM AT MACH 6.6

James Wayne Sawyer

Langley Research Center
Hampton, Va. 23665

NATIONAL AERONAUTICS AND SPACE ADMINISTRATION · WASHINGTON, D. C. · MAY 1977

TECH LIBRARY KAFB, NM
0134187

1. Report No.	2. Government Accession No.	3. Recipient's Catalog No.
NASA TN D-8415		

4. Title and Subtitle	5. Report Date
AEROTHERMAL AND STRUCTURAL PERFORMANCE OF A COBALT-BASE SUPERALLOY THERMAL PROTECTION SYSTEM AT MACH 6.6	May 1977
	6. Performing Organization Code

7. Author(s)	8. Performing Organization Report No.
James Wayne Sawyer	L-11286
	10. Work Unit No. 506-17-22-00
9. Performing Organization Name and Address NASA Langley Research Center Hampton, VA 23665	11. Contract or Grant No.
	13. Type of Report and Period Covered Technical Note
12. Sponsoring Agency Name and Address National Aeronautics and Space Administration Washington, DC 20546	14. Sponsoring Agency Code

15. Supplementary Notes

16. Abstract

A flightweight, metallic thermal protection system (TPS) applicable to reentry and hypersonic vehicles was subjected to multiple cycles of both radiant and aerothermal heating in order to evaluate its aerothermal performance and structural integrity. The TPS consisted of a 108.0-cm by 152.4-cm (42.5-in. by 60-in.) corrugation-stiffened skin and supports fabricated from a cobalt-based alloy (L-605), a 5-cm (2-in.) thick microquartz insulation blanket enclosed in an inconel foil, and a titanium sheet which simulated the vehicle primary structure. The TPS was subjected to 32 thermal tests, 13 of which were aerothermal tests conducted in the Langley 8-foot high-temperature structures tunnel at a nominal free-stream Mach number of 6.6. The TPS was heated by the radiant lamps for a cumulated total of 6.59 hours at a surface temperature of approximately 1145 K (2060° R) and was tested in the stream for a cumulated total of 423 sec. Good structural integrity and thermal performance were demonstrated by the TPS under both a radiant and aerothermal heating environment typical of a shuttle entry. The shingle-slip joints effectively allowed for thermal expansion of the panel without allowing any appreciable hot gas flow into the TPS cavity. The TPS also demonstrated good structural ruggedness.

17. Key Words (Suggested by Author(s))	18. Distribution Statement
Thermal protection system Hypersonic Corrugated surface Metallic heat shield	Unclassified - Unlimited Subject Category 39

19. Security Classif. (of this report)	20. Security Classif. (of this page)	21. No. of Pages	22. Price*
Unclassified	Unclassified	52	$4.50

*For sale by the National Technical Information Service, Springfield, Virginia 22161

AEROTHERMAL AND STRUCTURAL PERFORMANCE OF A COBALT-BASE SUPERALLOY THERMAL PROTECTION SYSTEM AT MACH 6.6

James Wayne Sawyer
Langley Research Center

SUMMARY

A flightweight, metallic thermal protection system (TPS) applicable to reentry and hypersonic vehicles was subjected to multiple cycles of both radiant and aerothermal heating in order to evaluate its aerothermal performance and structural integrity. The TPS consisted of a 108.0-cm by 152.4-cm (42.5-in. by 60-in.) corrugation-stiffened skin and supports fabricated from a cobalt-based alloy (L-605), a 5-cm (2-in.) thick microquartz insulation blanket enclosed in an inconel foil, and a titanium sheet which simulated the vehicle primary structure. The TPS was subjected to 32 thermal tests, 13 of which were aerothermal tests. All tests were conducted in the Langley 8-foot high-temperature structures tunnel with the corrugations aligned in the stream direction. For the aerothermal tests, the nominal free-stream Mach number was 6.6, and unit Reynolds number was 5.5×10^6/m (1.7×10^6/ft). The TPS was heated by the radiant lamps for a cumulated total of 6.59 hours at a surface temperature of approximately 1145 K (2060° R) and was tested in the stream for a cumulated total of 423 sec.

The TPS demonstrated good thermal protection under both a radiant and aerothermal heating environment representative of a shuttle entry. Structural integrity of the TPS was maintained throughout the test series. Structural ruggedness was demonstrated by the TPS when it suffered only minor damage upon being inadvertently subjected to uncontrolled rapid overheating and cooling, particle impact due to the stream, and arcing between the lamps and the panel with only minor damage. The shingle-slip joints effectively allowed for thermal expansion of the panel without allowing any appreciable hot gas flow into the TPS cavity.

INTRODUCTION

The cost of transportation to space by shuttle-type vehicles depends to a great extent on the effectiveness of the thermal protection systems (TPS). To minimize cost, the TPS must be fully reusable and have a long service life. The Langley Research Center has undertaken an extensive testing program to assess the thermal and structural performance of various TPS in a realistic aerothermal environment. Several full-scale TPS panels have been designed, fabricated, and tested as reported in references 1 to 5. Both external insulation concepts similar to that chosen for the space shuttle and metallic concepts suitable for advanced space transports or hypersonic vehicles are included. The results reported herein are for one of the metallic TPS in the test series.

The test panel consisted of a corrugation-stiffened metallic skin, standoff supports, and a microquartz insulation package. The skin and supports are fabricated from a cobalt-base material (L-605). The skin was attached to the standoffs by high-temperature bolts, and the assembly was bolted to a titanium sheet representative of a vehicle primary structure. The test assembly was designed and fabricated by Grumman Aerospace Corporation for application along a 1255 K (2260° R) isotherm on the shuttle orbiter. The panel was subjected to 32 thermal tests, 13 of which combined radiant and aerothermal heating test segments to represent an entry temperature history. All tests were conducted in the Langley 8-foot high-temperature structures tunnel. For the aerothermal tests, the free-stream Mach number was 6.6 and the unit Reynolds number was 5.5×10^6/m (1.7×10^6/ft).

Certain commercial materials are identified in this paper in order to specify adequately which materials were investigated in the research effort. In no case does such identification imply recommendation or endorsement of the product by NASA, nor does it imply that the materials are necessarily the only ones or the best ones available for the purpose. In many cases equivalent materials are available and would probably produce equivalent results.

SYMBOLS

Values are given in both SI Units and in U.S. Customary Units. The measurements and calculations were made in U.S. Customary Units.

M	Mach number
n	number of half-waves in y-direction over width of panel
p	pressure, Pa (psia)
q	dynamic pressure, Pa (psia)
$\dot{q}_c$	rate of heat transfer by conduction, W/m^2 (Btu/ft^2-sec)
$\dot{q}_r$	rate of heat transfer by radiation, W/m^2 (Btu/ft^2-sec)
R	unit Reynolds number
T	temperature, K ($^\circ$R)
t	time, sec
x,y,z	panel coordinates, cm (in.) (see fig. 9)
α	angle of attack, deg (see fig. 9)
Δp	differential pressure, positive in z-direction, Pa (psi)
δ	deflection, positive in z-direction, cm (in.)

ω frequency, Hz

Subscripts:

b panel-holder base

ι local conditions at edge of boundary layer

s surface

t total condition in combustor

∞ free stream

APPARATUS AND TESTS

Panel

Design criteria.- The thermal protection system considered in the present investigation was designed to protect primary structures from high surface temperatures during 100 entry cycles typical of those expected on the shuttle orbiter. The entry surface temperature and differential-pressure histories used in the present design are shown in figure 1. A peak surface temperature of 1260 K (2260° R) is obtained at 700 sec; at this time the surface differential pressure is approximately 1.9 kPa (40 psf). The maximum primary structure temperature is 500 K (900° R) and occurs at approximately 1200 sec. The critical design surface differential pressure occurs during ascent and is 20.7 kPa (432 psf).

General description.- The thermal protection system evaluated in the present investigation was designed and fabricated by Grumman Aerospace Corporation and is shown in figure 2. The system consisted of the following components: a corrugation-stiffened metallic skin, five rows of standoff supports, and a microquartz insulation package. The skin and supports were fabricated from a cobalt-based material (L-605). The skin was divided into two full bays and two half bays; each bay spanned the full width of the assembly. The full bays formed the center portion of the panel and the two half bays formed the leading and trailing edges of the panel. Shingle-slip joints were employed at the juncture of the center bays with the leading and trailing edges. High-temperature bolts were used to attach the panel skin to the standoffs so as to facilitate skin removal. The skin and the standoff assembly were bolted to a titanium sheet representative of the vehicle primary structure. The panel was 152.4 cm (60 in.) long by 108.0 cm (42.5 in.) wide. The mass of the various elements are itemized in table I where the total unit mass of the assembly is shown to be 13.23 kg/m^2 (2.71 lb/ft^2).

Detail design.- Cross-section details of the corrugation-stiffened skin are shown in figure 3. The corrugated outer sheet was 0.025 cm (0.010 in.) thick and had a cross-section shape composed of a series of circular arc segments separated by flats. The inner sheet was 0.020 cm (0.008 in.) thick and had trapezoidal corrugations. The two sheets were spot welded together along the flats.

The corrugations had a pitch of 3.81 cm (1.50 in.) and heights of 0.25 cm (0.10 in.) and 2.11 cm (0.83 in.) for the outer and inner sheets, respectively. The pitch-to-height ratios were sufficiently large to avoid thermal buckling of the corrugations. (See ref. 6.)

The individual bay skins were constructed in two segments approximately 51 cm (20 in.) square as shown by the photograph in figure 4. The flats on two adjacent skin segments were overlapped and bolted together to form a full bay width. The L-shaped clips shown in figure 4 were spot welded to the outer edge of the bay skin to provide part of the side-edge seals that will be discussed later. The studs shown attached to the corrugations in figure 4 were used to hold the thermal insulation in place. The outer surface of the skin was coated with a high-temperature (Pyromark) black paint in order to improve the thermal emittance of the surface.

The thermal insulation package consisted of 56 kg/m^3 (3.5 lb/ft^3) microquartz insulation and had a total thickness of 5.08 cm (2.0 in.). The insulation was enclosed in a 0.008-cm (0.003-in.) thick Inconel 600 foil package. The foil was overlapped at the edges and seam welded. The insulation under the full size panels was constructed in approximately 43- by 50-cm (17- by 20-in.) rectangular packages. (See fig. 5.) Small, foil-enclosed insulation packages shown in figure 5 were used to provide thermal protection around various supports. To prevent rupturing the packages, four 0.64-cm (0.25-in.) diameter vent holes were provided in the edges of the full-size packages and one hole was provided in each end of the small foil enclosures. The full-size insulation packages were held in place against the corrugated panel by 2.5-cm (1.0-in.) diameter retainer washers fastened to the studs shown in figure 4. The small insulation packages were held in place by the panel supports.

Two types of supports, each having a height of 8.10 cm (3.19 in.), were used to connect the panels to the primary structure. A photograph of the supports and their arrangement on the simulated-vehicle primary structure is shown in figure 6. Details of TPS supports are given in figure 7; the two shingle-slip joint supports and three drag supports used on the assembly are shown in detail in figures 7(a) and 7(b), respectively. The shingle-slip joint supports allow relatively free longitudinal movement of the panel ends while maintaining an overlapping joint to prevent hot gas from flowing between the panels. The shingle-slip joint supports were composed of 0.020-cm (0.008-in.) thick, corrugation-stiffened vertical webs with continuous mounting brackets seam welded to the base and individual surface attachment flanges riveted to the top of the webs. Anchor nuts were tack welded to the attachment flanges so that the panels could be mounted from the outside. The web corrugations served the dual purpose of stiffening the web and allowing for thermal expansion. The drag supports kept the center of the panel fixed relative to the primary structure. The drag supports were composed of a single 0.025-cm (0.01-in.) thick, corrugation-stiffened web with mounting brackets seam welded to the base and surface attachment flanges riveted to the top of the web. Anchor nuts were also tack welded to the attachment flanges as they were for the shingle-slip joint supports. The drag supports had streamwise stiffeners located every 26.7 cm (10.5 in.) spanwise in order to take any longitudinal drag or thermal loads. Four streamwise stiffeners were used across the span of each drag support (fig. 6).

The supports were attached to a 0.19-cm (0.075-in.) thick titanium sheet stiffened with three hat-shaped and two I-shaped spanwise channel stiffeners. The stiffened sheet simulated a vehicle primary structure. The locations of the channel stiffeners are shown in the photograph of the bottom side of the primary structure (fig. 8). The skin and support brackets, the titanium sheet, and the spanwise stiffeners were bolted together and were separated by two 0.32-cm (0.13-in.) thick fiberglass insulation strips between the parts. The fiberglass strips were used to insulate the supports from the primary structure. Four deflectometer support brackets were attached to two streamwise hat-shaped channels. Pressure transducers support brackets were attached near the leading and trailing edges of the panel.

Panel Holder

Description.- The TPS was mounted in the panel holder illustrated in figure 9. Details on the development of this test fixture are given in reference 7. The panel holder has a sharp leading edge, is rectangular in planform, 141 cm (55.4 in.) wide by 300 cm (118 in.) long, and is 30.5 cm (12 in.) deep. Exterior surfaces are covered with 2.54-cm (1.0-in.) thick Glasrock foam tiles which protect the internal structure from the aerodynamic heating environment produced in the wind tunnel. For wind-tunnel testing, the panel holder is sting mounted at its base. Test panels are mounted within a rectangular cavity 108 cm (42.5 in.) wide by 152 cm (60 in.) long located 102 cm (40 in.) downstream from the leading edge. Aerodynamic fences along the sides of the panel holder provide two-dimensional flow over the test area, and a boundary-layer trip near the leading edge generates turbulent flow over the panel surface. Surface pressures and aerodynamic heating rates were varied by pitching the panel holder. Differential-pressure loading of the panel is controlled by regulating the cavity pressure under the TPS. A positive pressure differential (pushing in on panel surface) is obtained by opening the vent doors shown in figure 9, and thus reducing the cavity pressure to the panel-holder base pressure. Negative pressure differentials (pushing out on panel surface) are obtained by closing the vent doors and pressurizing the cavity. Further details of the differential-pressure control system are described in reference 3.

TPS installation.- The TPS assembly was bolted to the steel channel mounting beams (fig. 9) which in turn were bolted to the leading- and trailing-edge walls of the cavity in the panel holder. Metal shims were used to position the assembly on the beams so that the flats at the leading edge were flush with the panel-holder surface. The trailing edge of the panel overlapped the panel-holder surface and the flats were pressed tightly against it. In figure 10, the TPS is shown installed in the panel holder in the test chamber of the wind tunnel.

Detail photographs of the TPS leading- and trailing-edge installations are shown in figures 11(a) and 11(b), respectively. The leading-edge fairing shown in figure 11(a) provides a rearward-facing step and overlaps the panel leading edge. The leading-edge fairing was split into three pieces, each of which were riveted to a continuous bar. Each piece was rigidly attached at one end and allowed free transverse movement over its length.

Figure 12 illustrates the panel-edge details; a cross-section view of the leading-edge fairing is shown in figure 12(a) and the side-edge seal is shown in figure 12(b). The side-edge seals consisted of an L-shaped clip with one leg spot welded to the panel and the other leg pressed against the panel-holder cavity wall. A fiberglass-covered steel cable and a cantilever spring were used to hold the clip against the panel-holder cavity. The cable and cantilever spring were continuous over the full length of the panel.

Instrumentation

The panel was instrumented with thermocouples, pressure orifices, and linear deflectometers. The general location of the various instrumentation is shown in figure 13(a) and detail locations of the thermocouples are given in figure 13(b). High-speed motion-picture cameras were used for photographing the panel during wind-tunnel tests, and still photography was used for recording panel surface appearance throughout the test series.

Panel temperatures were sensed by a total of 56 chromel-alumel thermocouples. Twenty of the thermocouples were located on the inside of the panel surface, three were located inside the thermal insulation, and the remainder were located on the primary structure and around the various supports. Detail views A-A and B-B show the location of the thermocouples around and on the various standoffs. View C-C shows the location of the thermocouples inside the thermal insulation and the remaining views D-D, E-E, and F-F indicate thermocouple locations on the panel surface, inconel foil, and the primary structure. All the thermocouple leads were enclosed in stainless-steel sheaths to protect them from high temperatures. The thermocouple junctures located on metal surfaces were formed by spot welding each of the leads to the surface approximately 0.08 cm (0.03 in.) apart. Other themocouple junctures were formed by welding the leads together to form a small bead.

Four static, linear, potential-type deflectometers were used to measure the deflections at the center of the panel bays at locations indicated in figure 13(a). The deflectometers were mounted on brackets (fig. 8) behind the primary structure to protect them from the high surface temperatures and were connected to the panel skin by means of wires which passed through the insulation. Tension was maintained in the wire by restoring springs inside the deflectometer. Each of the deflectometers had a displacement range of 2.54 cm (1.0 in.) and they were positioned so that deflections could be measured in each direction.

Surface pressures were measured at two orifices on the panel surface near the center of the leading and trailing edges (fig. 13(a)), at four orifices spaced around the periphery of the panel-holder cavity, and at one orifice in the Glasrock 8.57 cm (3.38 in.) upstream of the cavity leading edge. In addition, pressures were measured between the surface and the insulation, and behind the panel assembly. The panel-holder base pressure was also measured during each run. All these measurements were obtained using 0.15-cm (0.06-in.) inside-diameter stainless-steel orifice tubing connected to strain-gage pressure transducers. The transducers were located in the cavity behind the TPS so they would not be subjected to high temperatures.

Test Facility

The present tests were conducted in the Langley 8-foot high-temperature structures tunnel shown schematically in figure 14(a). This facility is a hypersonic blowdown wind tunnel that operates at a nominal Mach number of 7, at total pressures between 4.1 and 24.1 MPa (600 and 3500 psia), and at nominal total temperatures between 1390 and 2000 K (2500° and 3600° R). Corresponding free-stream Reynolds numbers are between 1×10^6 and 10×10^6/m (0.3×10^6 and 3.0×10^6/ft). Within the operating envelope bounded by these conditions, the aerodynamic pressures and heating rates encountered in flight at Mach 7 in the altitude range between 24 and 40 km (80 000 and 130 000 ft) are obtained. Other details on this test facility are reported in reference 3.

The test model is initially stored in a pod below the test stream (fig. 14(b)) to protect it from adverse tunnel startup transient and acoustic loads. The model is covered with acoustic baffles (fig. 14(c)) until the desired hypersonic flow conditions are established. The baffles are then retracted and the model rapidly inserted into the stream on a hydraulically actuated elevator capable of traveling the 2.1 m (7 ft) to the center of the stream in approximately 1.0 sec. A model pitch system provides a range of angles of attack up to $\pm 20°$. Prior to tunnel shutdown, the model is withdrawn from the stream and covered with the acoustic baffles. The baffles attenuate the acoustic energy from approximately 168 dB to 157 dB over the range of combustor pressure. Other details of the acoustic baffles are given in reference 3.

A heater system was used for both the static radiant tests and as a preheat for the aerothermal tests. The heater system consisted of quartz-lamp radiators mounted inside the acoustic-baffle boxes (fig. 14(c)). The radiant lamps were powered by an ignitron tube power supply and were controlled by a closed loop servo system to give the desired temperature histories. Surface temperatures above 1260 K (2260° R) can be obtained using the preheat system. A more detailed discussion of the preheat system is given in reference 3.

Tests

In order to observe the cumulative effects of cyclic heating, the TPS was subjected to thermal tests and radiant-preheat—aerothermal tests with temperature-time histories similar to those shown in figure 15. In both the thermal and aerothermal tests, radiant lamps were used to heat the panel to the test temperature at a rate of 2.8 K/sec (5° R/sec). The radiant-heat test temperature was chosen for most of the tests so that it would correspond to approximately the maximum surface temperature obtainable in the tunnel stream (1145 K (2060° R)) and thus is lower than the peak design temperature (1255 K (2260° R)). A few lower temperature tests were conducted near the beginning of the test series to check the panel and test equipment at lower thermal loads. For the thermal-cycle tests (fig. 15(a)), the maximum surface temperature was maintained for periods between 500 and 1200 sec, and then the surface was allowed to cool at a rate of 2.8 K/sec (5° R/sec) until natural cooling occurred at a lower rate. For the radiant-preheat—aerothermal tests (fig. 15(b)), the maximum preheat temperature was maintained for approximately 600 sec and then the TPS was exposed

to the tunnel stream for as long as possible at flow conditions that would maintain the preheat surface temperature of 1145 K (2060° R).

The procedure for the aerothermal part of the tests was to start the tunnel, obtain correct flow conditions, de-energize the quartz lamps, retract the lamps and acoustic baffles, and insert and simultaneously pitch the panel holder so that it attained the desired angle of attack on reaching the stream center line. At the end of the aerodynamic exposure the procedure was reversed, and tunnel shutdown was initiated after the lamps and acoustic baffles covered the panel. Following the aerodynamic exposure, the panel was allowed to cool naturally (uncontrolled). The time elapse between the lamps being de-energized and the panel entering the stream was kept to a minimum and was approximately 5 sec.

Data Acquisition

During thermal tests and preheat events, thermocouple and deflectometer outputs were recorded at 2-sec intervals. When the wind tunnel was operating, thermocouple, deflectometer, and pressure-transducer outputs were recorded at a rate of 20 samples per sec. Analytical quantities reported herein for the wind-tunnel tests are based on the thermal, transport, and flow properties of the combustion-products test medium as determined from reference 8. Results from tunnel-stream survey tests were used (ref. 7) to determine free-stream conditions in the test section from reference measurements in the combustion chamber. Local Mach number was obtained from oblique-shock relations.

TPS CHARACTERIZATION

The present investigation focused on TPS structural and thermal response during repeated exposures to both radiant and aerodynamic heating. Structural integrity was monitored during the test series by means of visual inspections, topographical surface mapping, and vibration surveys. The thermal response was evaluated by comparing the measured temperature distributions through the panel and insulation system with that obtained from a thermal analysis.

Structural Response

TPS static-load deflection data and vibration modes and frequencies were obtained experimentally before and after the heating tests and intermittently during the test program. For static-load deflections, the TPS was uniformly loaded with a differential pressure obtained by covering the panel surface with a vinyl sheet, sealing the edges to the panel-holder surface, and then reducing the pressure in the cavity under the TPS. Panel deflections were recorded at 1.4-kPa (0.2-psi) pressure increments up to a maximum differential pressure of 6.9 kPa (1 psi) using a deflectometer and traversing mechanism that can survey the entire TPS surface. (For further details, see ref. 4.)

The vibration mode-and-frequency survey was conducted by exciting the panel using an electromagnetic shaker mounted on the outside surface of the panel. Mode shapes were defined by surveying the entire panel surface with the

deflectometer and traversing mechanism used during the static-load deflection tests. Resonant frequencies were indicated by peak amplitudes obtained when sweeping the frequency of the shaker from 50 to 500 Hz. The location of the shaker and deflectometer were varied so as to detect the resonant frequencies of interest.

Thermal Analysis

A thermal analysis was made to determine the temperatures through the depth of the panel for comparison with the experimental results. The finite-difference program MITAS (Martin Interactive Thermal Analysis System) was used for the thermal analysis and is described in reference 9. The temperature-dependent thermal properties used for the TPS materials are tabulated in table II and were assumed to vary linearly between given temperatures.

A schematic of the section modeled and the heat-transfer modes considered in the thermal analysis are shown in figure 16. Due to symmetry, only one-dimensional heat flow was considered entering or leaving the modeled region. The surface temperature was assumed to be uniform and is provided as input to the analysis as a function of time. Heat was assumed to be radiated and conducted from the panel surface to the foil, radiated from the foil to the insulation, conducted through the insulation to the second foil, and then radiated from the foil to the primary structure where it was stored.

RESULTS AND DISCUSSION

Summary of Panel Tests

The panel was subjected to a total of 32 simulated reentry thermal cycles. Of these, 19 were radiantly heated thermal tests and 13 were aerothermal tests with radiant preheating. A summary of tests is given in table III. The order of testing and nominal test surface temperatures are included. For five of the thermal tests (2, 4, 5, 7, and 8), the surface temperature was maintained at approximately 810 K (1460° R), whereas for the other thermal and aerothermal tests the surface temperature was maintained at approximately 1145 K (2060° R). Also shown in table III are the exposure times at peak surface temperatures during both thermal and aerothermal tests. The TPS was subjected to the elevated test temperatures for a total of 6.59 hours and the Mach 6.6 stream for 423 sec.

Several events occurred during the test series which subjected the TPS to unusual load conditions. During test 5, severe arcing occurred between the lamp bank and a small area on the surface of the test panel. This arcing caused lamp failure and a rapid cooling of the panel surface. The arcing and subsequent rapid cooling resulted in flaking of the high-temperature paint on the panel surface, discoloration and pitting of the surface, and a small crack in the panel surface in the affected area. Although the arcing occurred near the beginning of the test series, no further deterioration of the affected surface area occurred during the remainder of the tests.

During thermal tests 10 and 14, inadvertent loss of control of the heat lamps resulted in rapid heating of the panel surface to about 1480 K (2660° R). When the lamps were brought under control, the surface rapidly cooled to 1145 K (2060° R). The resulting high-temperature spikes are shown in figure 17 where a summary of the surface temperature-time histories for all tests are given. The high-temperature spikes did not cause any visible structural damage or significant changes in the natural vibration frequencies of the TPS, but did result in cracking and deterioration of the high-temperature paint coating.

The panel was also subjected to impacts from very small particles in the test stream which were produced by the flaking of an aluminum oxide coating on the facility combustor lining. The particles had sufficient velocity and mass to dent the plate surface and at a few locations penetrated the outer surface layer. However, the particle impacts did not cause any serious degradation of the panel.

The aerothermal test conditions and exposure times are summarized in table IV; the free-stream and local-flow conditions are tabulated along with the pressure differential across the panel surface, the base pressure of the panel holder, and the calculated unit Reynolds number. During each aerothermal test, the differential pressure across the panel surface was held relatively constant except as noted in table IV, but from test to test it varied from 8.62 kPa (1.25 psi) acting inward to 4.82 kPa (0.7 psi) acting outward.

TPS Thermal Performance

Thermal tests.- Typical thermal performance of the panel when it was exposed to radiant heating is demonstrated in figure 18 for test 3. Temperature-time distributions through the center of one of the panels, along a shingle-slip joint and support, and along a drag support are shown in this figure. The insets show the locations of the various thermocouples. The panel surface was heated at a nominal rate of 2.8 K/sec (5° R/sec) to 1145 K (2060° R) and maintained at that temperature for approximately 400 sec. The surface temperatures shown in figures 18(a) and 18(b) differ by approximately 33 K (60° R), thus indicating some variations in the surface heating. The primary-structure temperatures continue to increase even after the surface temperature is decreased and reach a maximum temperature of approximately 405 K (730° R) at 1300 sec.

Temperature profiles calculated using the MITAS program are shown in figure 18(a) for comparison with the measured profiles through the center of the TPS. The surface-temperature distribution shown in figure 18(a) for thermocouple 4 was used as input in making the theoretical calculations. The measured and calculated profiles inside the insulation and on the primary structure show good agreement over the complete thermal cycle and thus verify the adequacy of the thermal model. Since this thermal model was used to predict the primary-structure design temperature given in figure 1, those predicted temperatures should be fairly accurate, thus demonstrating that the panel provides good thermal protection for the primary structure. In fact, for the design heating cycle given in figure 1, the primary-structure temperatures are low enough that an aluminum primary structure could be used.

The temperature profiles presented in figures 18(a), 18(b), and 18(c) show similar variations at each location. This situation may be seen more clearly in figure 19 where the temperature is shown as a function of the depth from the panel surface after 750 sec. Temperature distributions are shown through the center of the panel (triangular symbols), along the shingle-slip joint and support (circular symbols), and along the drag support (square symbols). The temperature distributions at the various locations fall within the narrow band shown by the shaded area, thus indicating that the supports do not provide a significant heat short to the primary structure.

Aerothermal tests.- As noted previously, for 13 of the 32 tests the TPS was inserted into a Mach 6.6 stream for several seconds of aerothermal heating. In each of these tests, the TPS was pitched at an angle of attack to the stream that would produce a surface temperature approximately the same as that produced by the radiant preheaters. In addition, the pitching of the panel holder increased the local static pressure and provided a differential pressure across the panel.

Figure 20 shows the environment imposed on the TPS panel during test 15; figure 20(a) is a typical surface-temperature profile, and figure 20(b) gives histories of the surface temperature, the differential pressure across the panel, and the angle of attack of the panel holder for the aerothermal portion of the test. The sequence of events during the aerothermal portion of the test is noted in the figure. The panel was maintained at a constant elevated temperature for approximately 600 sec before the TPS was inserted into the stream. The TPS remained in the stream for 40 sec at an angle of attack of 12.2°. A pressure differential of approximately 8.3 kPa (1.2 psi) pushed in on the panel during the first half of the test, and it decreased to 4.1 kPa (0.6 psi) for the remainder of the test. This large change in differential pressure resulted from a slight change in the free-stream flow conditions which changed the shock pattern on the panel-holder strut and caused the base and cavity pressure of the panel holder to increase. The small variations in the differential pressure during the first half of the test are due to the unsteadiness of the base and cavity pressure of the panel holder. Note that a reduction in the surface temperature occurred from the time the power to the lamps was cut to the time when the TPS was inserted in the stream, but the surface temperature recovered quickly once it was exposed to the aerodynamic heating. After the TPS was withdrawn from the stream, it was allowed to cool naturally (uncontrolled).

Panel-joint effectiveness.- An important factor in the design of metallic thermal protection systems is the effectiveness of the individual panel joints in preventing hot gas flow into the TPS cavity. For the present design, the shingle-slip joint is of interest since it must allow for thermal expansion as well as prevent hot gas ingress.

The effectiveness of the shingle-slip joint in preventing hot gas ingress is indicated in figure 21. Temperature distributions through the center of the TPS 25.4 cm (10.0 in.) away from any joint (triangular symbols) are compared with the distributions at a shingle-slip joint support (circular symbols). Temperature distributions are shown at approximately equivalent times in the heating history for tests 3, 11, and 15. The temperature distribution obtained for test 3 (solid symbols) is for a thermal cycle. The temperature distributions

shown for tests 11 and 15 (open symbols) were obtained during the aerothermal portion of the tests when the pressure differentials acting inward were 2.90 kPa (0.42 psi) and 4.82 kPa (0.70 psi), respectively. For all three tests, the temperature distributions through the center of the TPS and through the shingle-slip joint are in good agreement. Thus, even for substantial pressure differentials there is no evidence of hot gas flowing through the shingle-slip joint.

Thermal deformations.- Since the panel is corrugation stiffened, rapid heating and cooling results in significant thermal deformations. The thermal deflection at the center of one of the panels, the surface temperature, and the temperature differential between the two surfaces are shown as a function of time in figure 22 for thermal test 3. During the initial panel heatup, the temperature differential reached 75 K (135° R) and the panel bowed out to approximately 0.75 cm (0.3 in.). As the panel surface temperature stabilized, the temperature differential went to zero, and the panel returned to a flat state. This behavior suggests that the shingle-slip joint supports (figs. 6 and 7(a)) offer little resistance to thermal expansion. During panel cool down the temperature differential became negative which caused the panel to bow inward by approximately 0.50 cm (0.2 in.). As the panel cooled, the temperature differential decreased, and the panel deflection again approached zero.

Panel Integrity

Thermal.- The thermal integrity of the TPS remained good throughout the tests as indicated in figure 23 - a comparison of the temperature histories obtained near the beginning and near the end of the test series. The figure shows temperature histories for tests 3 and 27 at several locations through the panel thickness. The good agreement between the two temperature distributions for thermocouple 54 located inside the insulation indicates that no degradation of the insulation material occurred during the tests.

Structural.- Panel structural integrity can be assessed by comparing the natural frequencies and static-load deflections obtained before and after the test series. The first (lowest) five natural frequencies obtained for one bay before and after the test series are shown in figure 24. The frequencies are shown as a function of the number of half-waves in the transverse direction. The frequencies show only minor differences before and after the test series. Static-load deflections were also found to be in good agreement before and after the test series, thus indicating the good structural integrity of the panel.

Posttest condition of panel.- Except for the appearance of the panel surface, the TPS was in excellent structural condition at the conclusion of the test series. Figure 25 consists of photographs of the panel surface taken before and after the test series. The overall discoloration pattern on the panel surface shown in figure 25(b) was produced by uneven heating of the quartz-lamp radiators during preheating and thermal cycling events. The distinct darker and lighter spots near the longitudinal center line of the panel and on the upper left-hand quarter of the panel are due to contaminants which dropped on the panel while it was being heated - probably drops of hydraulic fluid or grease. The discoloration and surface damage caused by the arcing between the lamps and the surface are identified in the figure. At the end of the test

series, almost all the high-temperature paint was gone from the panel surface, and the panel surface had developed a relatively uniform oxidized coating.

Figure 26 is a view of the shingle-slip joint near the side edge of the panel after tests. The light-shaded rub marks indicate the distance the two surfaces overlap when heated to the test temperature. The panel length grew approximately 1.5 percent and such growth is consistent with calculated values for the 1145 K (2060° R) heatup. The shingle-slip joints were able to accommodate the panel thermal growth without any apparent adverse effects. Some lateral shifting of the top surfaces is evident and was probably due to thermal buckling of the L-shaped clip on the side-edge seals (fig. 12(b)). Recall that the side-edge seals were required to install the panel in the test fixture and are not part of the actual panel design. Nevertheless, the apparent distortion at the shingle-slip joint had no measurable effect on the panel performance.

Figure 27 shows posttest closeup views of some damaged areas on the surface of the panel. Figure 27(a) shows a crack in the panel surface, a melted panel edge, and a local buckle; each was noted after test 5 during which arcing occurred between the radiant lamps and the panel. The hole in the panel surface shown in figure 27(b) was due to particle impingement from the stream. Numerous dents and a few other small holes in the panel surface due to particle impact during the test series were also obtained. Neither the arcing nor particle-impact damage caused any noticeable deterioration of the structural or thermal protection capability of the TPS, and none of the damaged areas showed evidence of further deterioration during the remainder of the test series. Thus, the tests demonstrated a high level of durability and damage tolerance for the TPS.

The TPS was disassembled in order to inspect interior parts for signs of deterioration. The bolts which attached the panel to the standoffs had seized in the nuts but could be removed by twisting off the heads. Inspection of the disassembled TPS showed no evidence of failure of any component parts. The posttest conditions of the insulation package may be seen in figure 28. The inconel foil enclosing the insulation oxidized considerably, but it was still completely intact and showed no other signs of deterioration. The oxidation occurred only near the hot surface of the panel where the temperatures exceeded 1090 K (1960° R).

CONCLUDING REMARKS

A flightweight, metallic thermal protection system (TPS) applicable to reentry and hypersonic vehicles was subjected to multiple cycles of both radiant and aerothermal heating in order to evaluate its aerothermal performance and structural integrity. The TPS consisted of a 108.0-cm by 152.4-cm (42.5-in. by 60-in.) corrugation-stiffened skin and supports fabricated from a cobalt-based alloy (L-605), a 5-cm (2-in.) thick microquartz insulation blanket enclosed in an inconel foil, and a titanium sheet which simulated the vehicle primary structure. The TPS was subjected to 32 thermal tests, 13 of which were aerothermal tests conducted in the Langley 8-foot high-temperature structures tunnel at a nominal free-stream Mach number of 6.6. The TPS was heated by the radiant lamps for a total of 6.59 hours at a surface temperature of approximately 1145 K (2060° R) and was tested in the stream for a total of 423 sec.

The TPS demonstrated good thermal protection under both a radiant and aerothermal heating environment representative of a shuttle entry. Structural integrity of the TPS was maintained throughout the test series. In addition, structural ruggedness was demonstrated by the TPS when it suffered only minor damage upon being inadvertently subjected to uncontrolled rapid overheating and cooling, particle impact due to the stream, and arcing between the lamps and the panel. The shingle-slip joints also effectively allowed for thermal expansion of the panel without allowing any appreciable hot gas flow into the TPS cavity.

Langley Research Center
National Aeronautics and Space Administration
Hampton, VA 23665
February 14, 1977

REFERENCES

1. Hunt, L. Roane; Shideler, John L.; and Weinstein, Irving: Performance of LI-1542 Reusable Surface Insulation System in a Hypersonic Stream. NASA TN D-8150, 1976.

2. Hunt, L. Roane: Performance of a Mullite Reusable Surface Insulation System in a Hypersonic Stream. NASA TM X-3397, 1976.

3. Deveikis, William D.; Bruce, Walter E., Jr.; and Karns, John R.: Techniques for Aerothermal Tests of Large, Flightweight Thermal Protection Panels in a Mach 7 Wind Tunnel. NASA TM X-71983, 1974.

4. Deveikis, William D.; Miserentino, Robert; Weinstein, Irving; and Shideler, John L.: Aerothermal Performance and Structural Integrity of a René 41 Thermal Protection System at Mach 6.6. NASA TN D-7943, 1975.

5. Bohon, Herman L.; Sawyer, J. Wayne; Hunt, L. Roane; and Weinstein, Irving: Performance of Full Size Metallic and RSI Thermal Protection Systems in a Mach 7 Environment. AIAA Paper No. 75-800, May 1975.

6. Anderson, Melvin S.; and Stroud, C. W.: Experimental Observations of Aerodynamic and Heating Tests on Insulating Heat Shields. NASA TN D-1237, 1962.

7. Deveikis, William D.; and Hunt, L. Roane: Loading and Heating of a Large Flat Plate at Mach 7 in the Langley 8-Foot High-Temperature Structures Tunnel. NASA TN D-7275, 1973.

8. Leyhe, Edward W.; and Howell, Robert R.: Calculation Procedure for Thermodynamic, Transport, and Flow Properties of the Combustion Products of a Hydrocarbon Fuel Mixture Burned in Air With Results for Ethylene-Air and Methane-Air Mixtures. NASA TN D-914, 1962.

9. Martin Interactive Thermal Analyzer System - Version 1.0. User's Manual. MDS-SPLPD-71-FD238 (REV 3), Martin Marietta Corp., Mar. 1972.

TABLE I.- MASS OF TPS ELEMENTS

Detail parts	Mass		Unit mass	
	kg	lbm	kg/m^2	lbm/ft^2
Panel:				
Corrugated skin	4.18	9.21	2.54	0.52
Corrugations	5.30	11.69	3.22	0.66
Total	9.48	20.90	5.76	1.18
Supports:				
Rib standoffs	0.72	1.59	0.44	0.09
Clip and angles	2.17	4.78	1.32	0.27
Support pads	0.32	0.71	0.19	0.04
Attaching hardware	1.36	3.01	0.83	0.17
Drag supports	0.24	0.53	0.15	0.03
Total	4.81	10.62	2.93	0.60
Insulation system:				
Insulation	4.66	10.27	2.83	0.58
Inconel foil bagging	1.77	3.90	1.07	0.22
Supports and retainers	1.04	2.30	0.64	0.13
Total	7.47	16.47	4.54	0.93
Total	21.76	47.99	13.23	2.71

TABLE II.- THERMAL PROPERTIES OF TPS MATERIALS

Material	Temperature		Conductivity		Temperature		Specific heat		Emissivity
	K	^oR	$\frac{W}{m-K}$	$\frac{Btu-ft}{ft^2-sec-^oR}$	K	^oR	$\frac{J}{kg-K}$	$\frac{Btu}{lb-^oR}$	
L-605	297	535	8.648	0.001389	297	535	368.11	0.0880	0.87
	1260	2260	28.368	.004556	1367	2460	533.34	.1275	
Inconel	297	535	9.439	0.001516	297	535	418.31	0.100	0.87
	775	1395	18.306	.002940	1260	2260	418.31	.100	
	1260	2260	29.333	.004711					
Titanium	297	535	6.488	0.001042	297	535	554.26	0.1325	----
	1144	2060	17.727	.002847	589	1060	610.73	.1460	
					922	1660	775.96	.1855	
Microquartz	297	535	0.045	0.00000722	297	535	778.05	0.186	----
	666	1200	.092	.00001472	489	880	978.84	.234	
	1260	2260	.247	.0000397	767	1380	1129.43	.270	
					1260	2260	1234.00	.295	

TABLE III.- SUMMARY OF TESTS

Test	Type of test	Nominal test surface temperature		Time at peak surface temperature, sec	
		K	°R	Thermal	Aerothermal
1	Thermal	1033	1860	1096	----
2	Thermal	811	1460	1986	----
3	Thermal	1145	2060	402	----
4	Thermal	811	1460	485	----
5	Thermal	[a]811	1460	447	----
6	Thermal	1145	2060	1068	----
7	Aerothermal	811	1460	420	42.0
8	Aerothermal	811	1460	430	38.5
9	Thermal	1145	2060	710	----
10	Thermal	[b]1467	2640	----	----
11	Aerothermal	1145	2060	561	28.5
12	Thermal	1145	2060	1035	----
13	Aerothermal	1145	2060	585	35.0
14	Thermal	[b]1478	2660	----	----
15	Aerothermal	1145	2060	606	40.0
16	Aerothermal	1145	2060	748	32.0
17	Aerothermal	1145	2060	657	30.2
18	Thermal	1145	2060	1080	----
19	Thermal	1145	2060	1005	----
20	Aerothermal	1145	2060	576	41.0
21	Thermal	1145	2060	1042	----
22	Aerothermal	1145	2060	604	38.0
23	Thermal	1145	2060	875	----
24	Thermal	1145	2060	653	----
25	Thermal	1145	2060	1208	----
26	Thermal	1145	2060	1252	----
27	Thermal	1145	2060	1170	----
28	Thermal	1145	2060	626	----
29	Aerothermal	1145	2060	443	17.0
30	Aerothermal	1145	2060	480	28.8
31	Aerothermal	1145	2060	590	22.0
32	Aerothermal	1145	2060	466	30.1
		Total time		23 306	423.1

[a]Arcing from lamps to panel.
[b]Uncontrolled heating.

TABLE IV.- AEROTHERMAL TEST CONDITIONS

Test	α, deg	T_t		p_t		p_∞		q_∞		M_∞	M_l	p_l		q_l		Δp		p_b		R	
		K	°R	MPa	psi	kPa	psi	kPa	psi			kPa	psi	kPa	psi	kPa	psi	Pa	psi	per m	per ft
7	0	1778	3200	16.92	2454	2.151	0.312	60.67	8.80	6.48	6.48	2.14	0.31	60.67	8.80	0.689	-0.10	2.21	0.32	5.38×10^6	1.64×10^6
8	-5.1, -9.0	1763	3174	16.93	2456	2.164	.314	59.71	8.66	6.47	5.00	7.24	1.05	123.00	17.84	-0.14, -4.62	-0.02, -0.67	1.38, 2.21	0.20, 0.32	5.41	1.65
11	-13.18	1689	3041	16.94	2458	2.199	.319	60.40	8.76	6.33	4.50	11.86	1.72	161.32	23.40	2.90	.42	6.55	.95	5.84	1.78
13	-12.06	1757	3162	17.10	2480	2.199	.319	61.43	8.91	6.45	4.63	10.62	1.54	151.75	22.01	2.27	.33	7.45	1.08	5.51	1.68
15	-12.16	1762	3172	17.04	2471	2.192	.318	61.23	8.88	6.45	4.63	10.55	1.53	151.27	21.94	8.62, 4.82	1.25, 0.70	1.10, 7.16	0.16, 1.14	5.44	1.66
16	-11.83	1649	2969	16.90	2451	2.199	.319	59.50	8.63	6.25	4.55	10.20	1.48	142.03	20.60	3.38	.49	8.00	1.16	6.07	1.85
17	-11.93	1761	3170	16.92	2454	2.164	.314	59.64	8.65	6.47	4.59	10.14	1.47	144.10	20.90	2.90	.42	8.00	1.16	5.45	1.66
20	-12.03	1811	3260	17.04	2471	2.158	.313	62.60	9.08	6.51	4.63	10.76	1.56	153.55	22.27	4.21	.61	8.27	1.20	5.25	1.60
22	-12.08	1794	3228	17.06	2475	2.171	.315	61.91	8.98	6.49	4.63	10.69	1.55	152.37	22.10	6.89, -2.00	1.0, -0.29	7.79	1.13	5.35	1.63
29	-12.31	1644	2960	17.01	2467	2.675	.388	71.71	10.40	6.24	4.55	12.89	1.87	182.02	26.40	6.89, -2.20	1.0, -0.32	8.39	1.21	6.10	1.85
30	-12.34	1781	3206	16.70	2423	2.137	.310	60.12	8.72	6.48	4.55	10.55	1.53	146.38	21.23	5.86, -0.90	0.85, -0.13	8.27	1.20	5.35	1.63
31	-12.46	1778	3200	17.13	2484	2.178	.316	61.43	8.91	6.48	4.55	10.76	1.56	149.69	21.71	6.21, -2.07	0.90, -0.30	8.27	1.20	5.45	1.66
32	-12.43	1641	2953	17.02	2469	2.220	.322	59.85	8.68	6.24	4.50	10.76	1.56	145.76	21.14	5.52, -1.38	0.80, -0.20	8.34	1.21	6.14	1.87

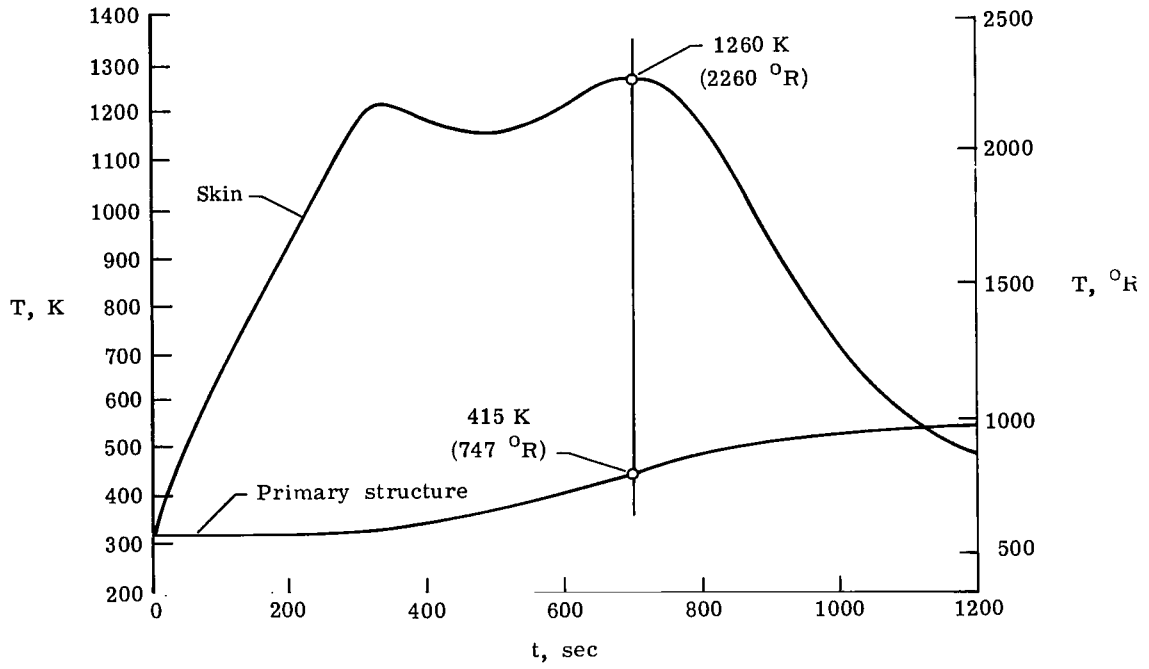

(a) Temperature history.

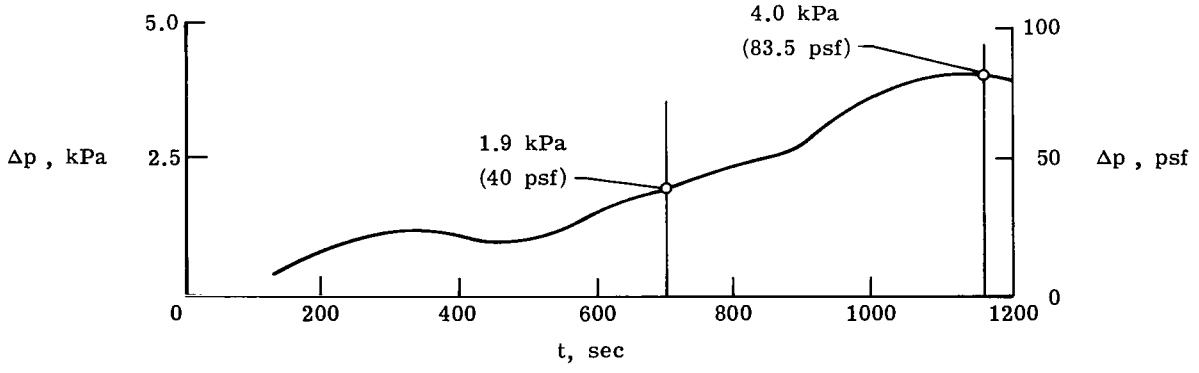

(b) Differential pressure history.

Figure 1.- Panel-entry-surface temperature and differential pressure for design conditions.

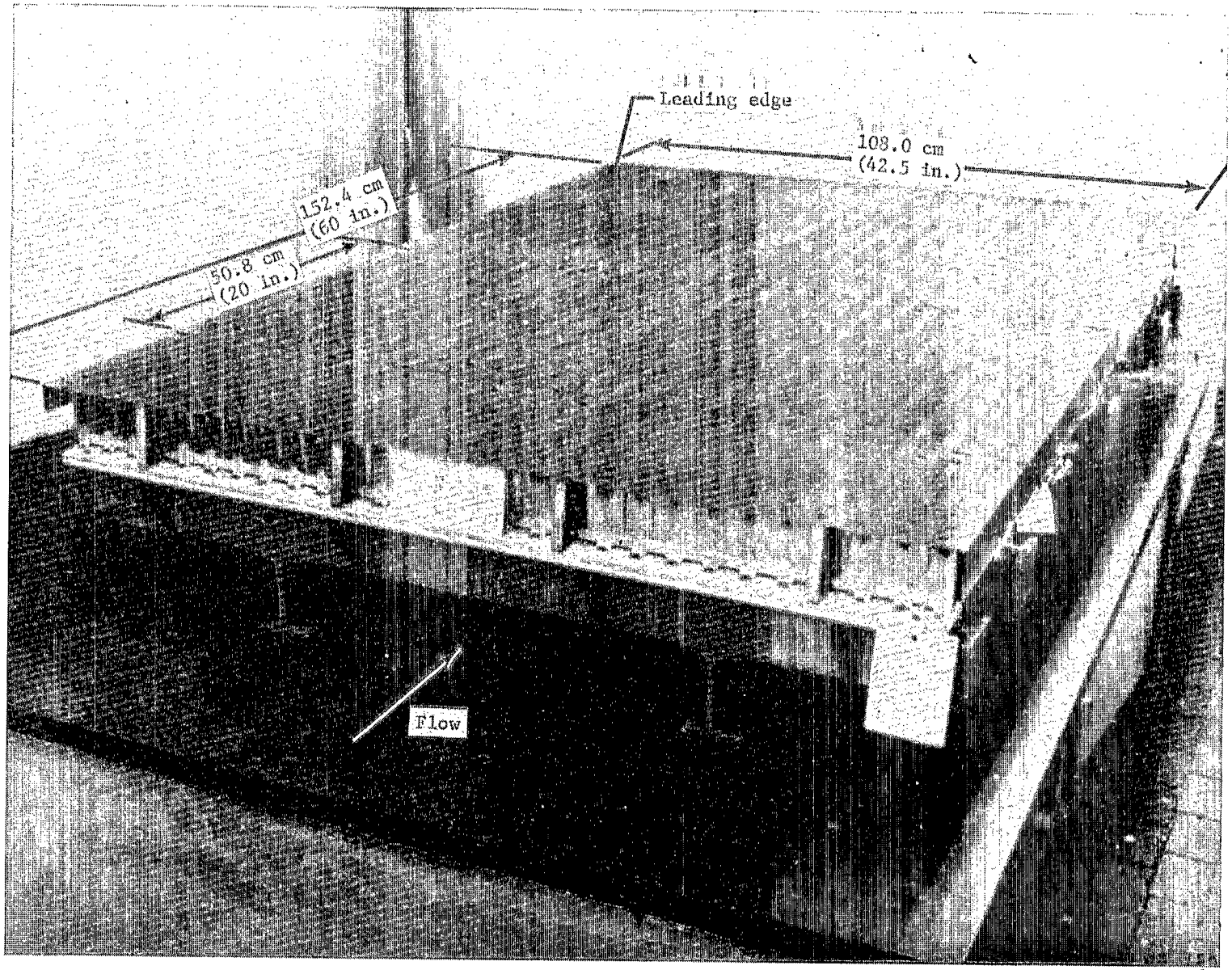

L-77-160

Figure 2.- Thermal protection system test panel.

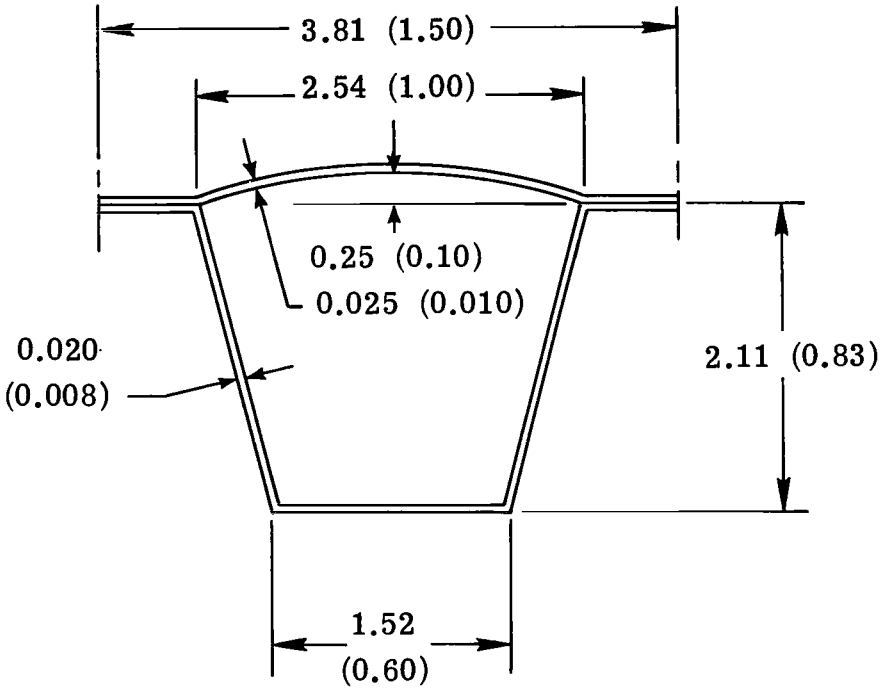

Figure 3.- Geometry of corrugation-stiffened panel. Dimensions are in cm (in.).

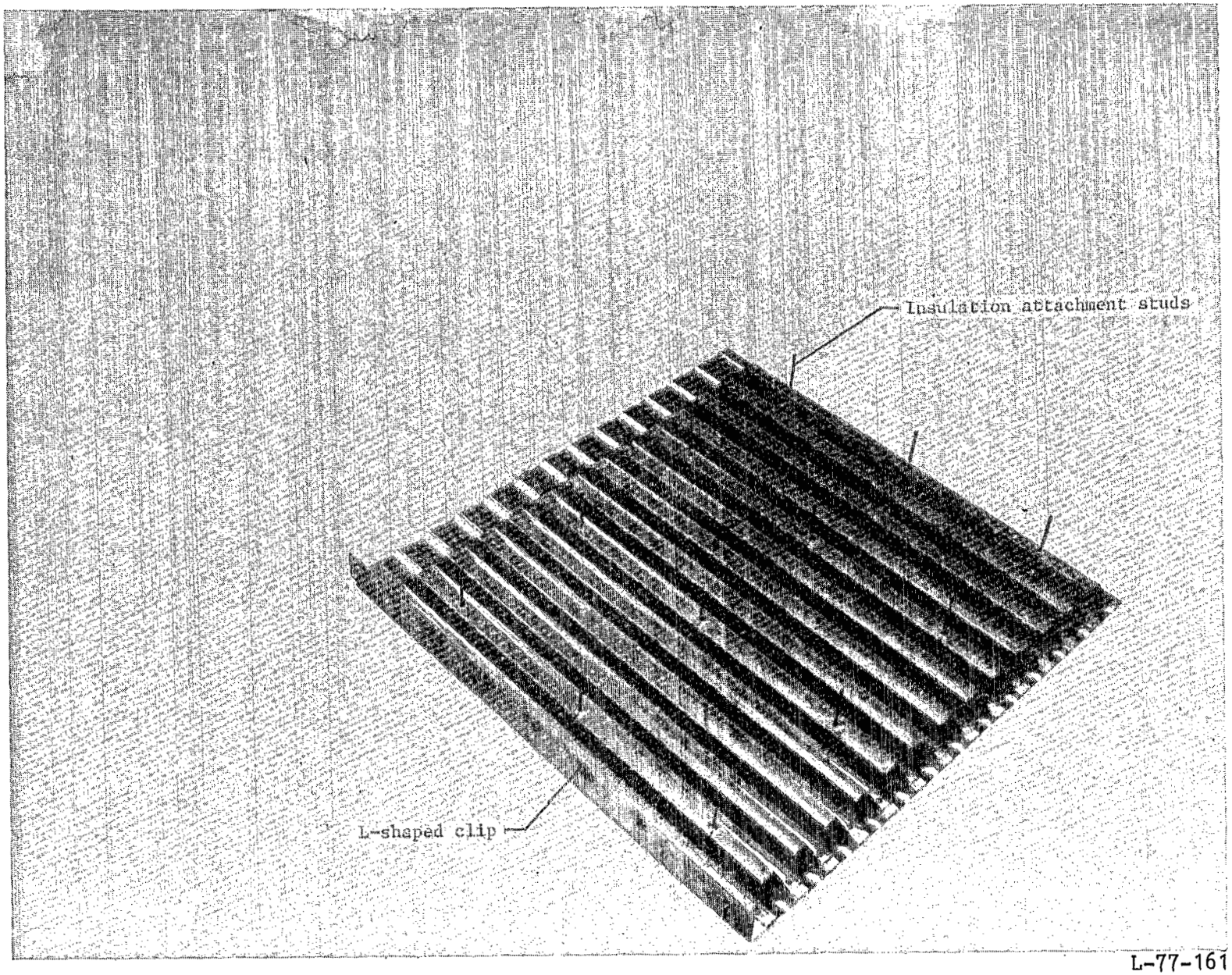

Figure 4.- Photograph of a section of the panel surface.

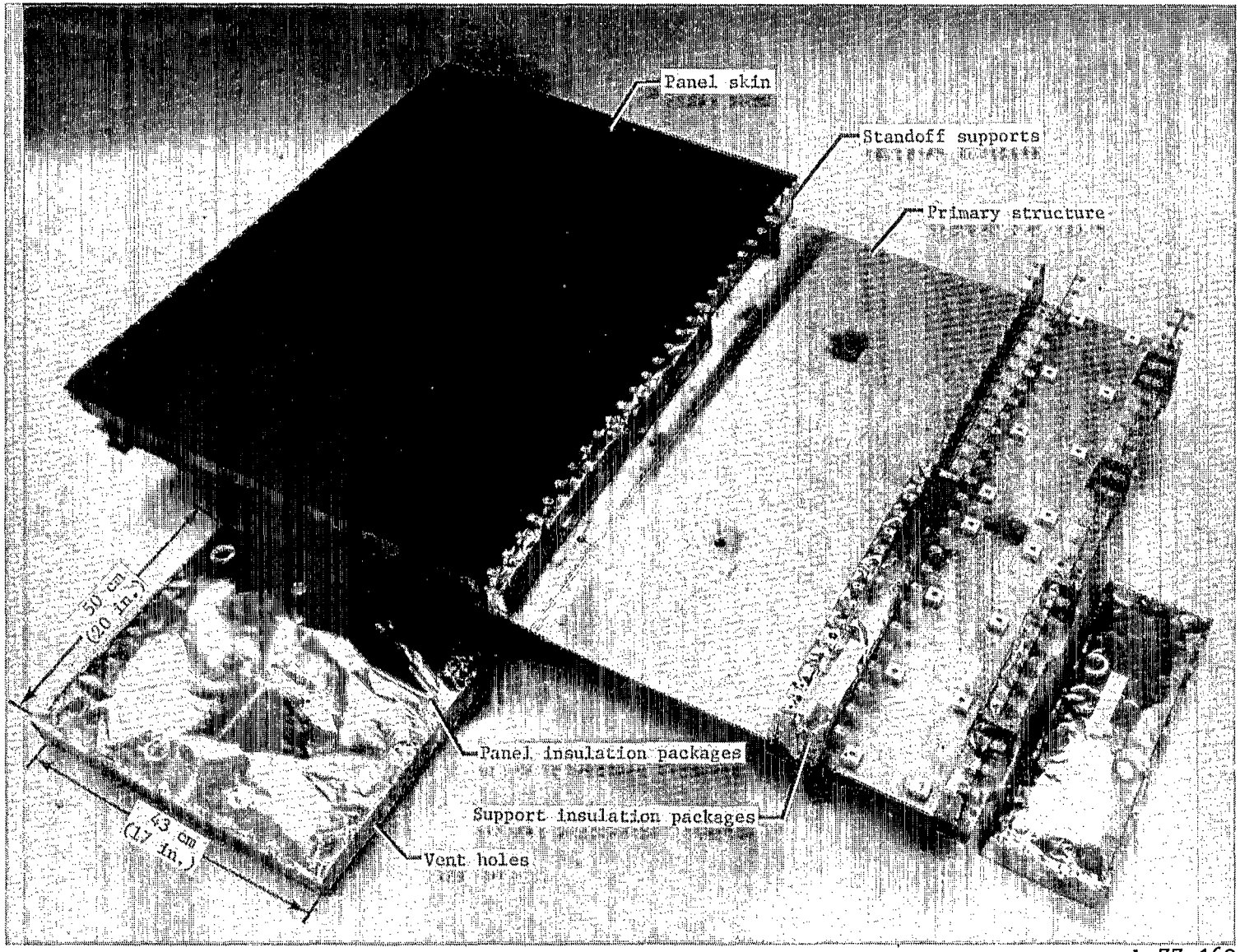

L-77-162

Figure 5.- TPS thermal insulation packages.

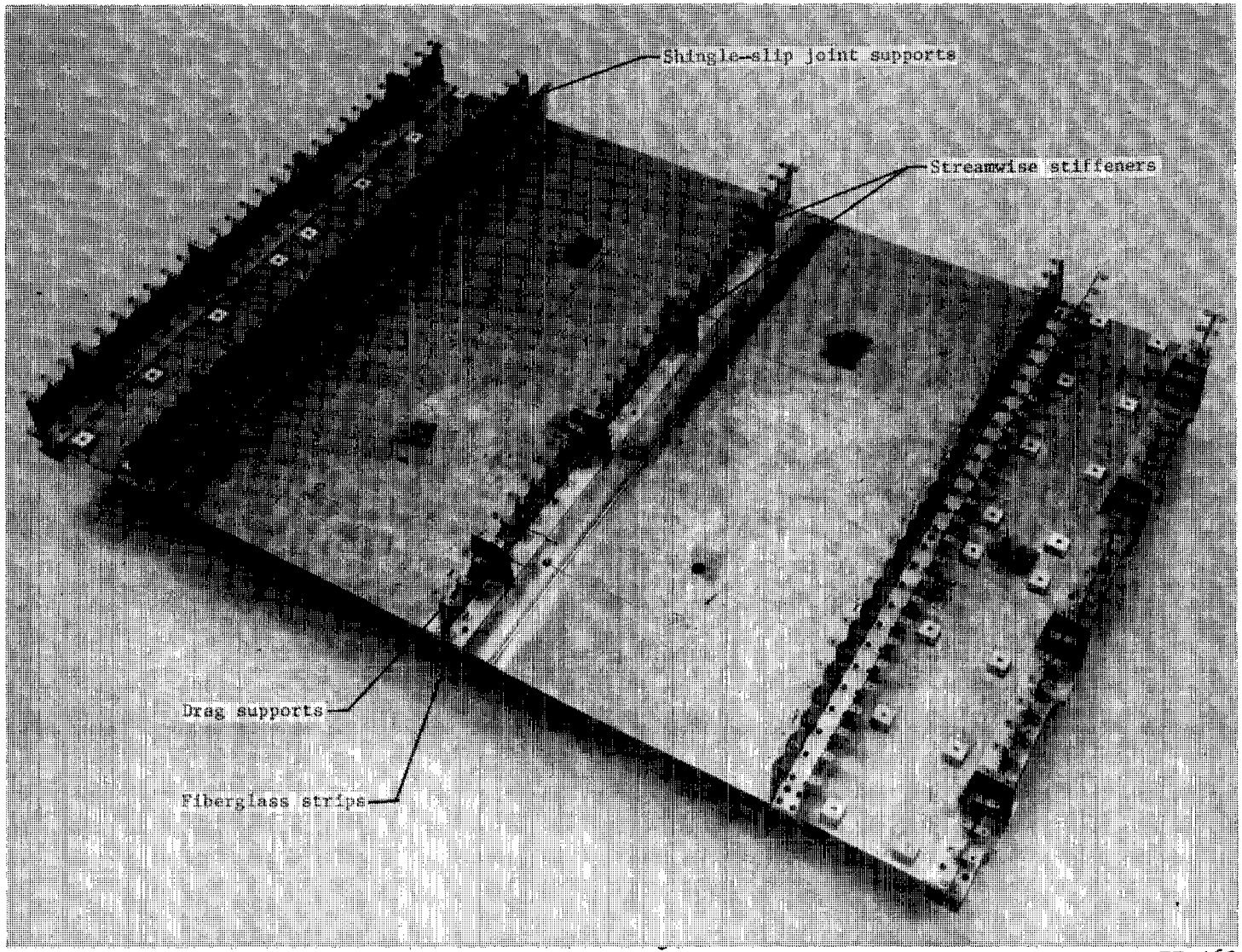

L-77-163

Figure 6.- Surface supports mounted on simulated-vehicle primary structure.

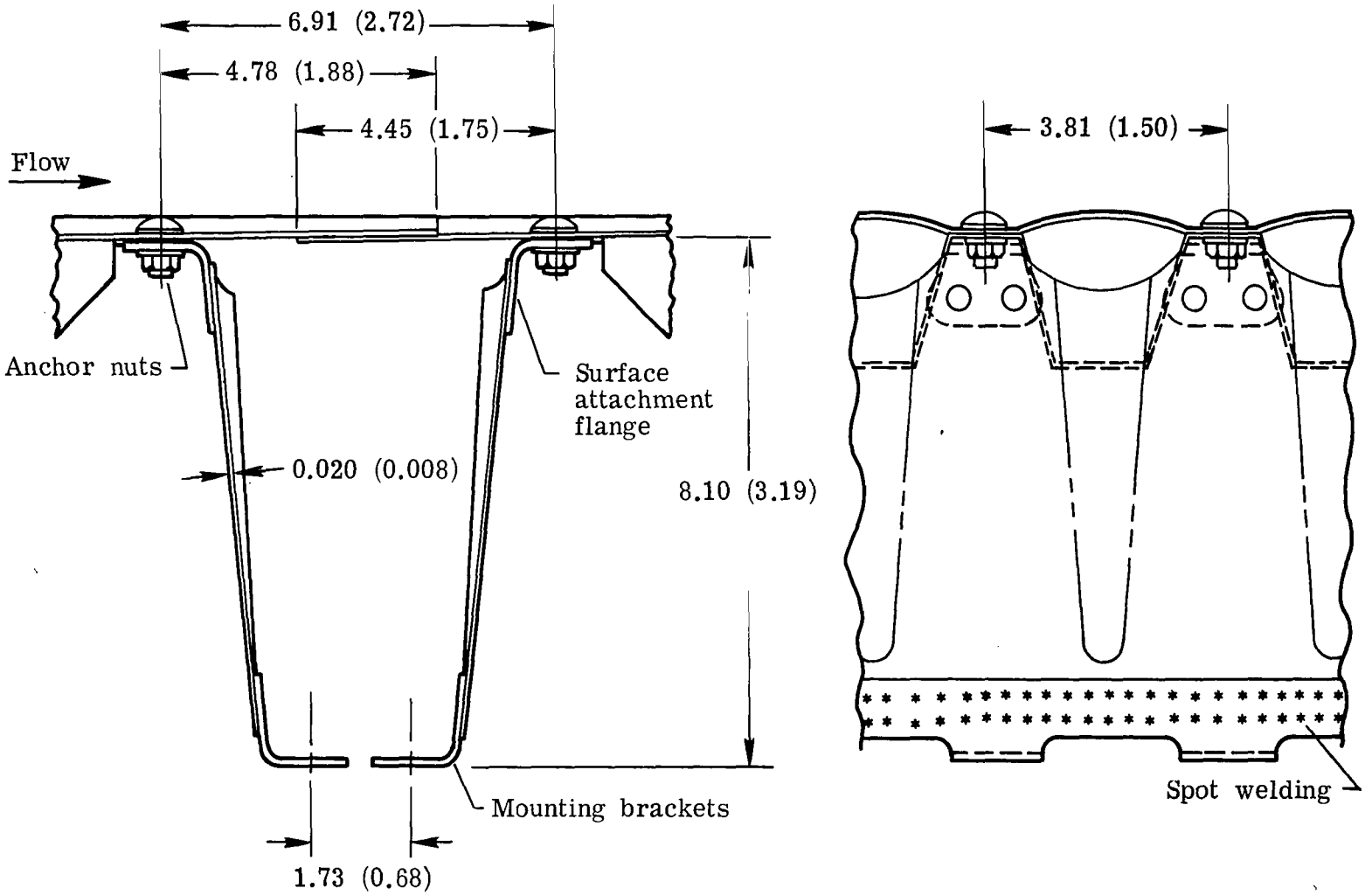

(a) Shingle-slip joint supports.

Figure 7.- Details of TPS supports. Dimensions are in cm (in.).

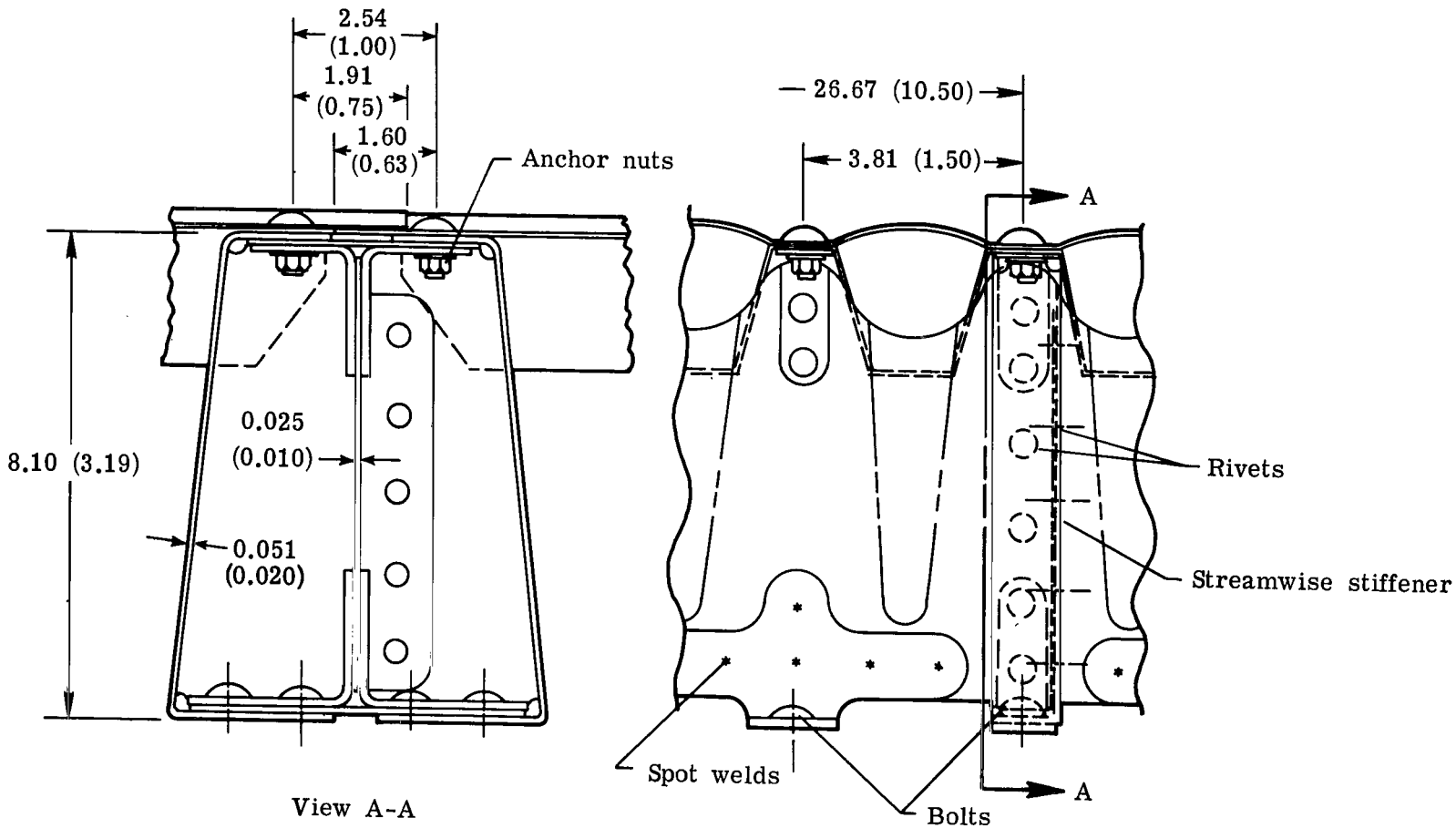

(b) Drag supports.

Figure 7.- Concluded.

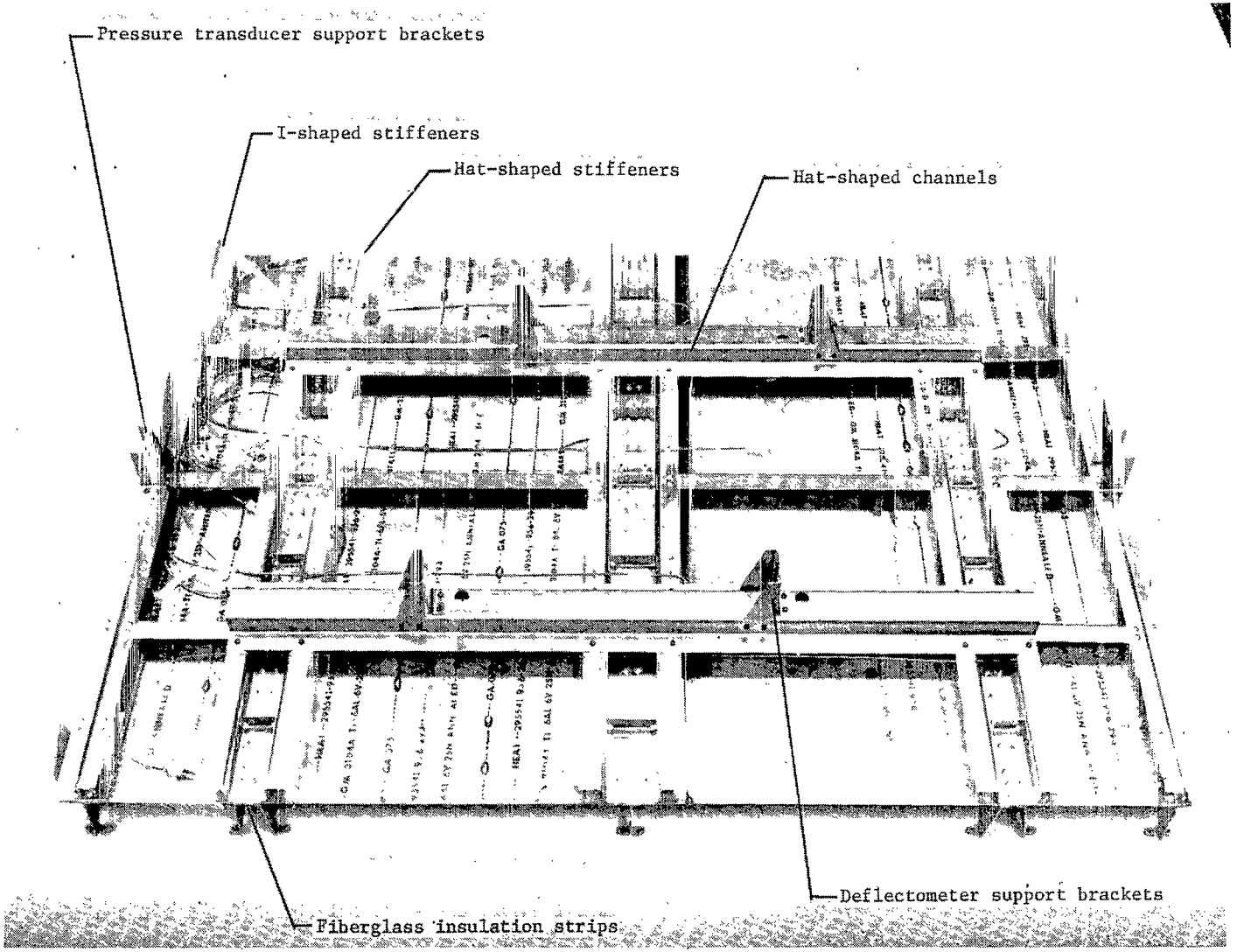

L-77-164

Figure 8.- Bottom side of TPS test assembly.

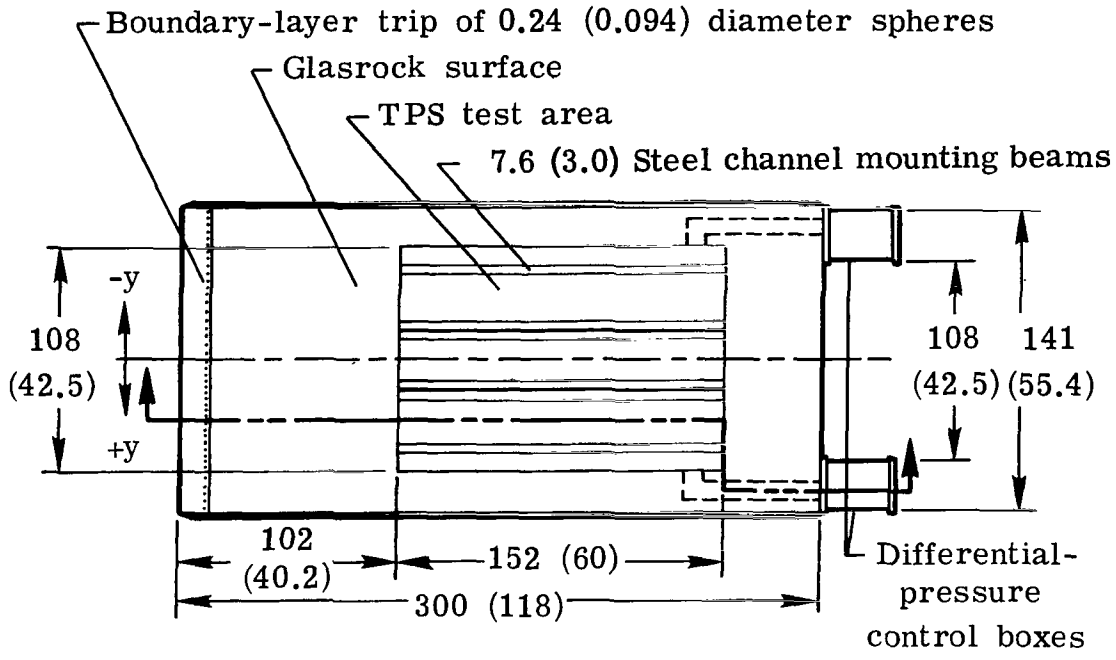

(a) Planview without TPS.

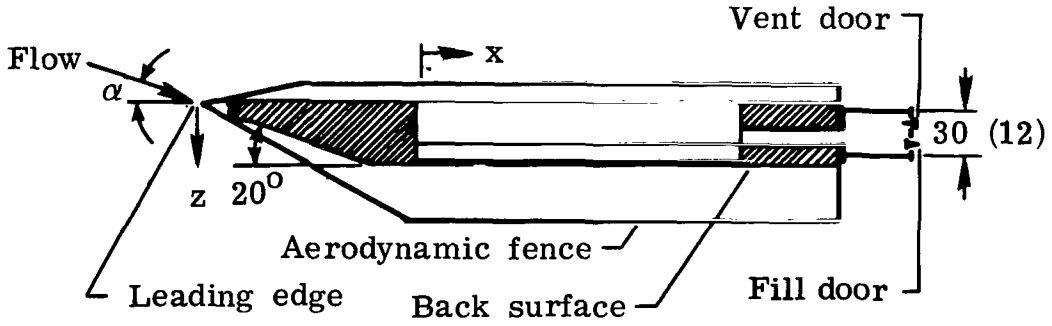

(b) Longitudinal cross section.

Figure 9.- Details of panel holder. Dimensions are in cm (in.).

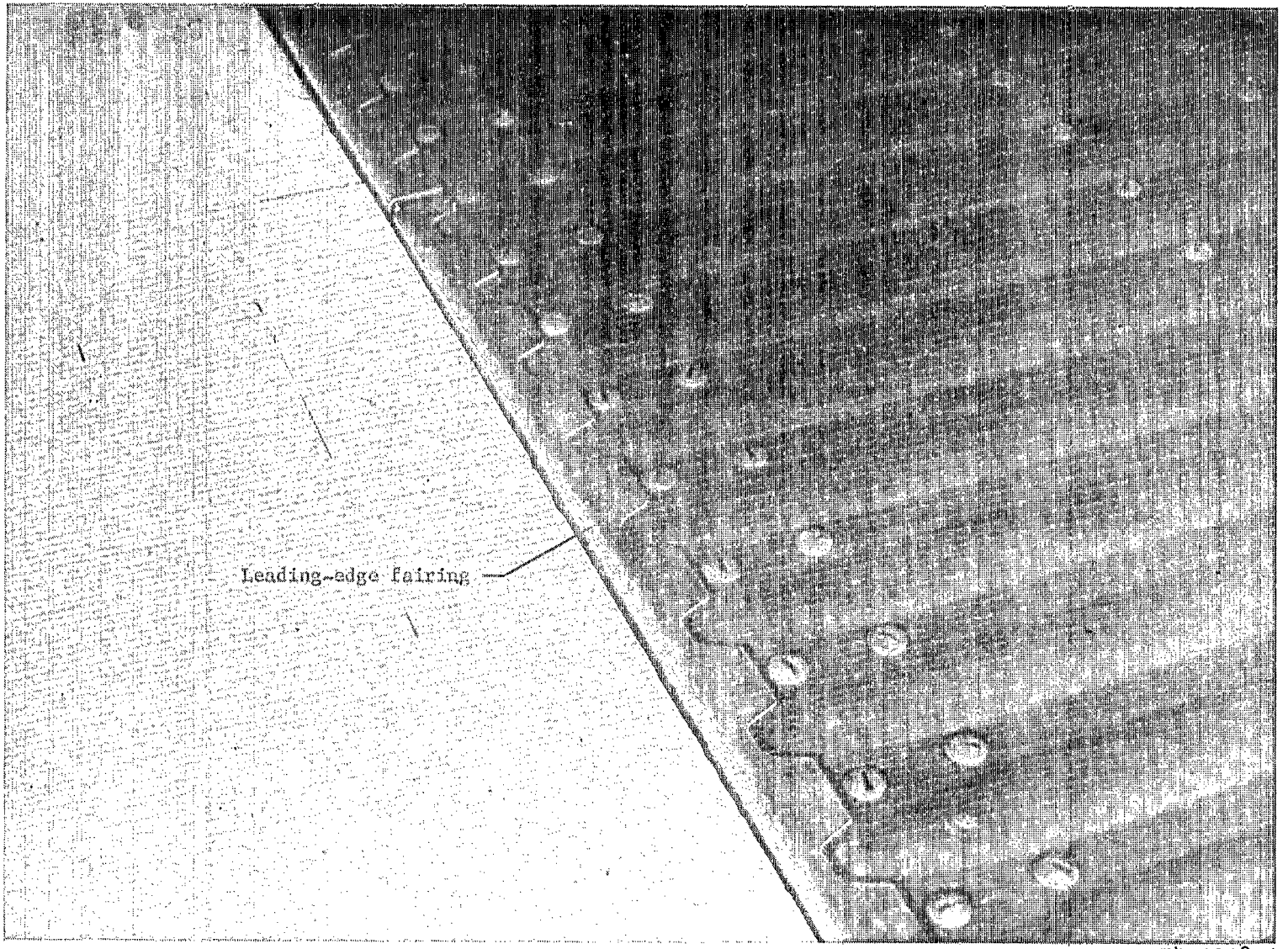

(a) Leading edge of panel.

Figure 11.- TPS edge fairings.

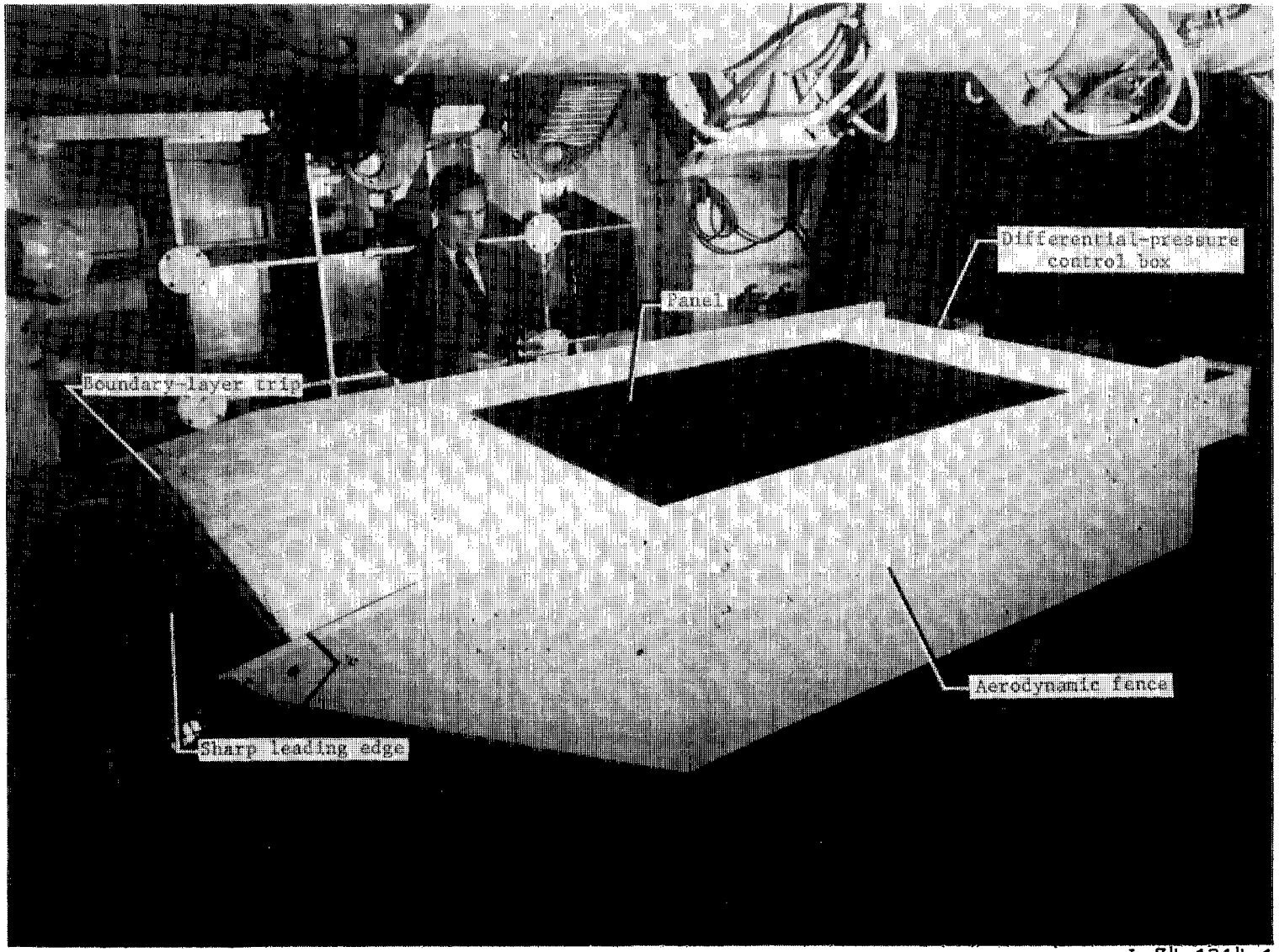

L-74-1314.1

Figure 10.- Typical panel installation in panel holder in wind tunnel.

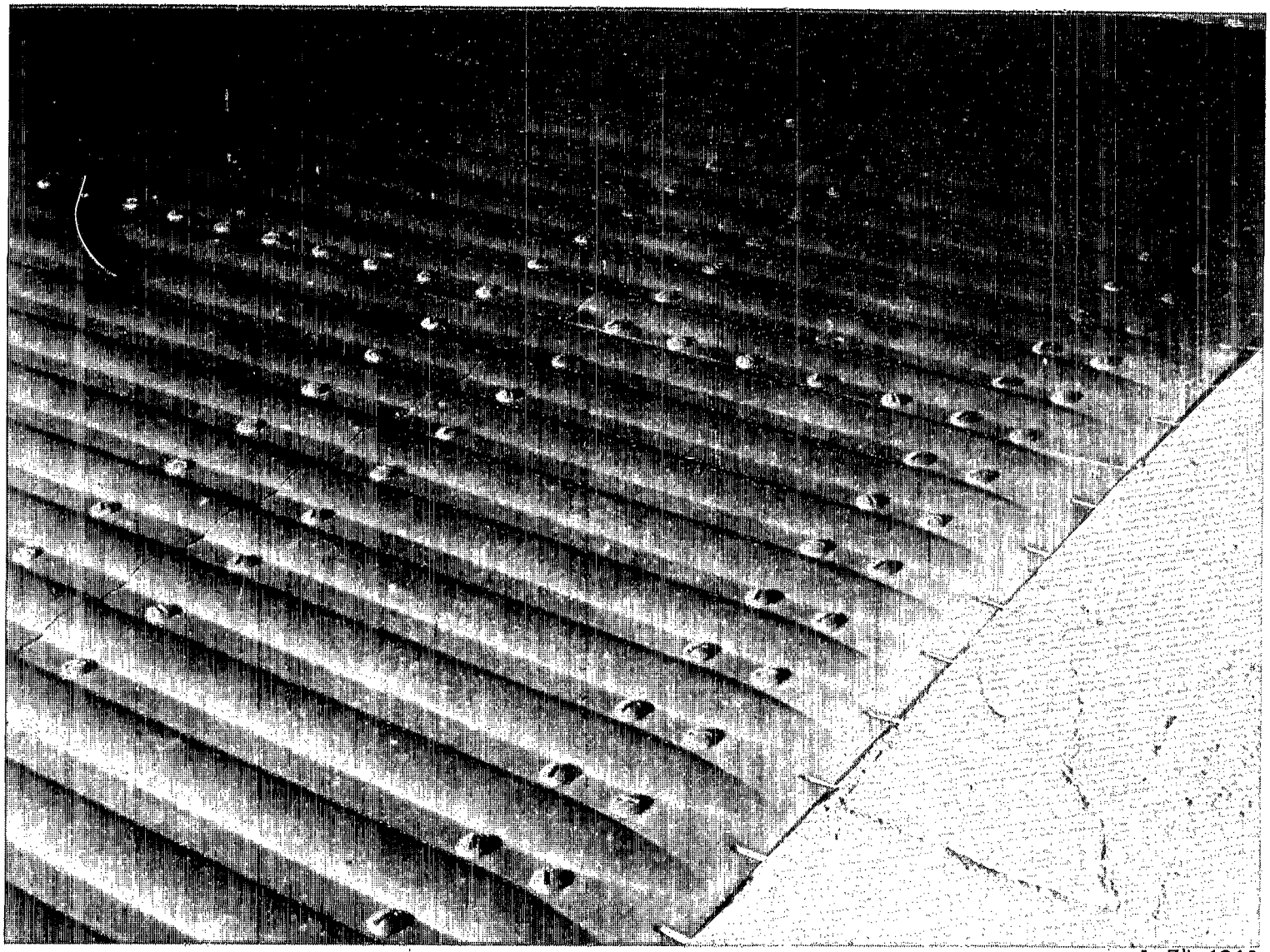

L-74-1319

(b) Trailing edge of panel.

Figure 11.- Concluded.

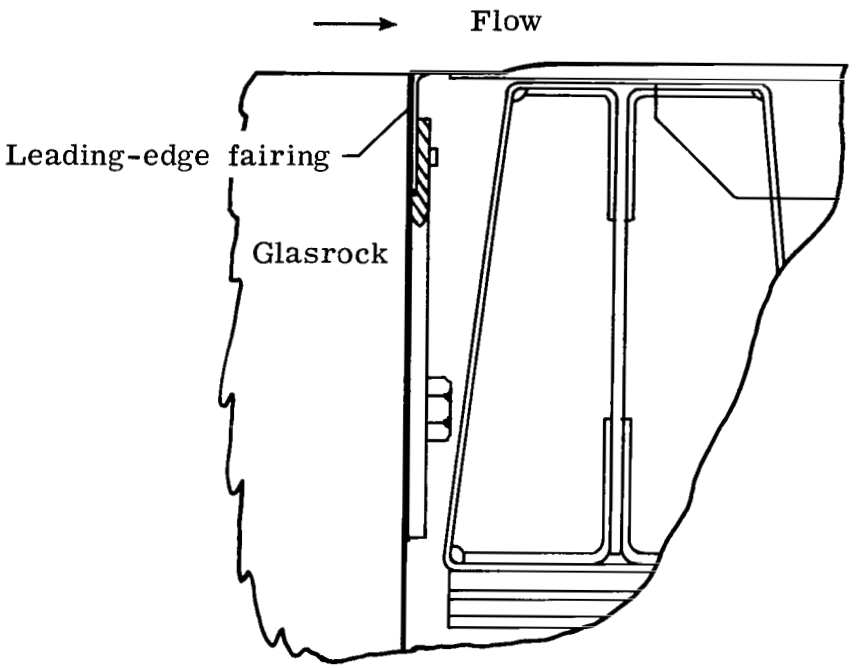

(a) Leading-edge fairing.

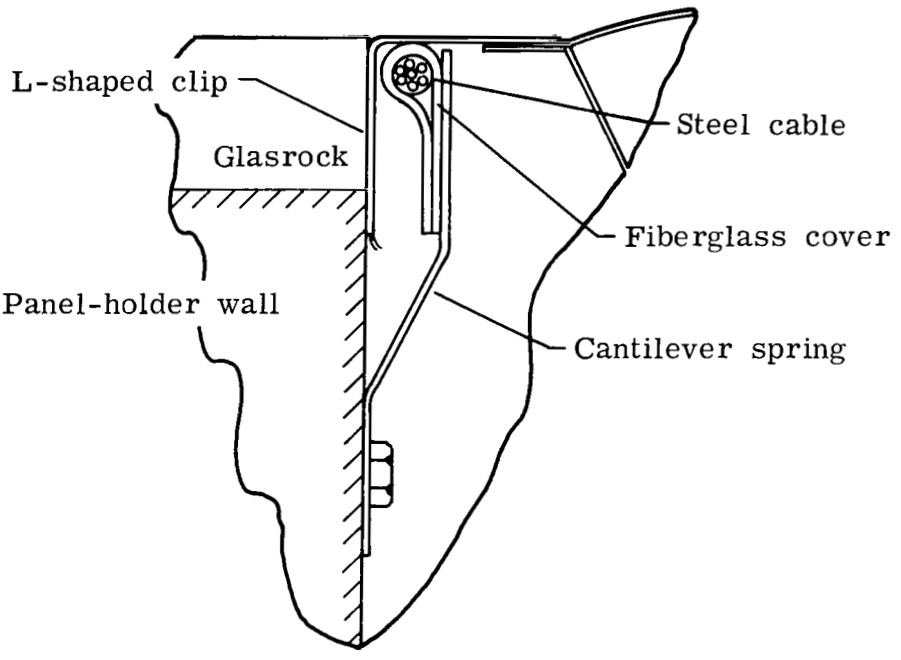

(b) Side-edge seal.

Figure 12.- Panel-edge details at interface with test apparatus.

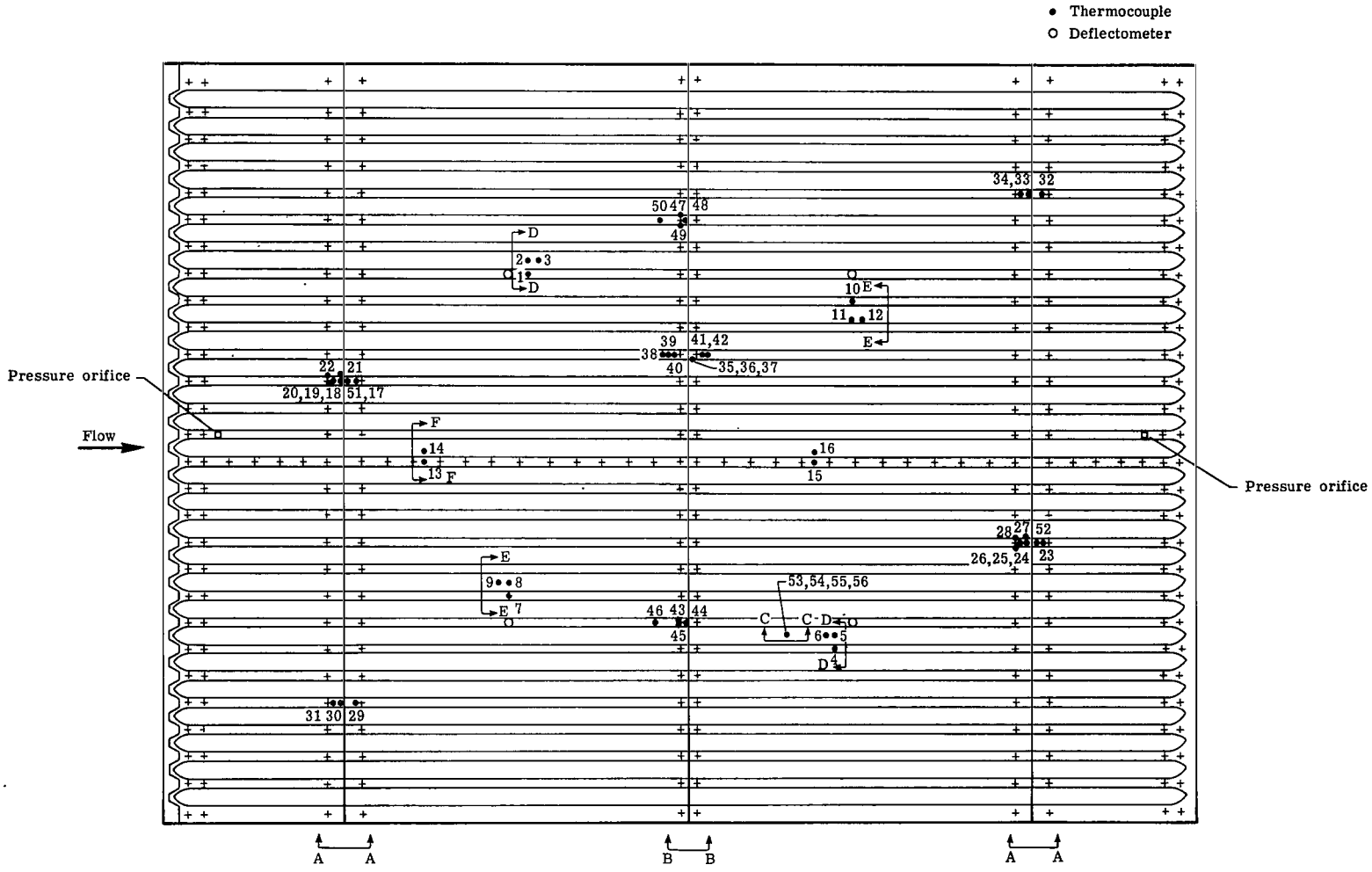

(a) General location of instrumentation.

Figure 13.- Location of instrumentation on test panel. Dimensions are in cm (in.).

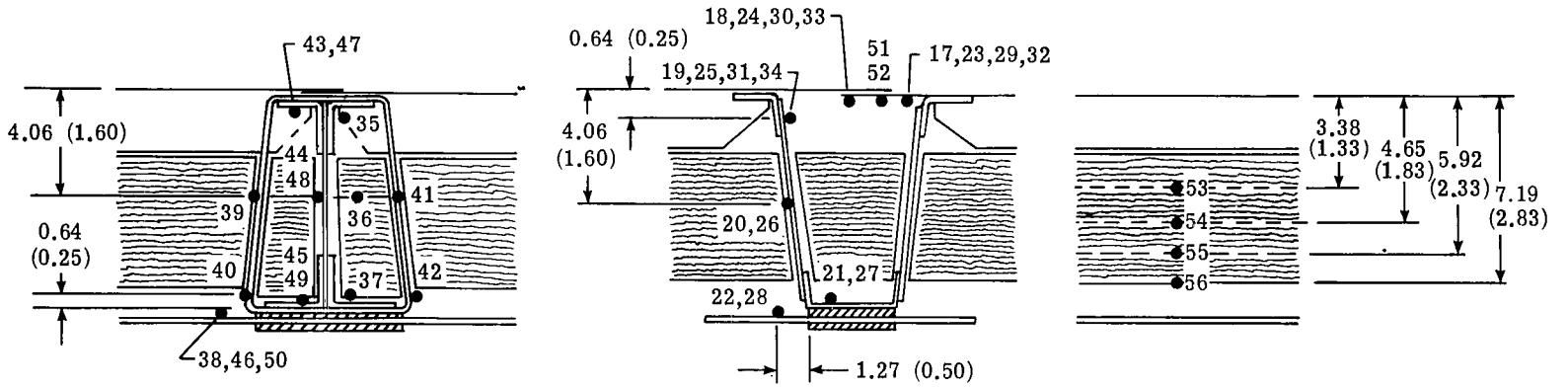

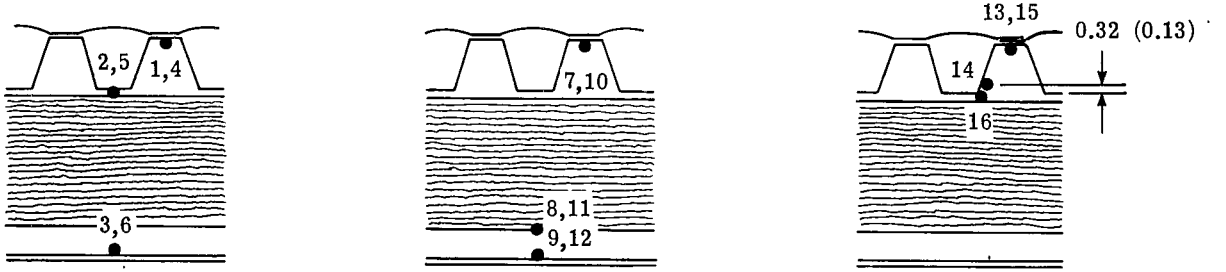

(b) Thermocouple locations.

Figure 13.- Concluded.

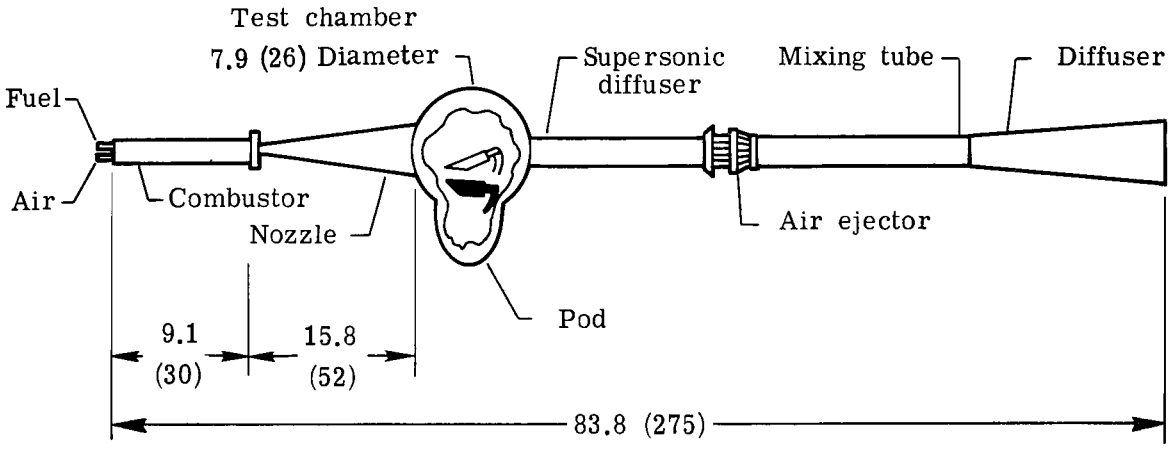

(a) Schematic of tunnel.

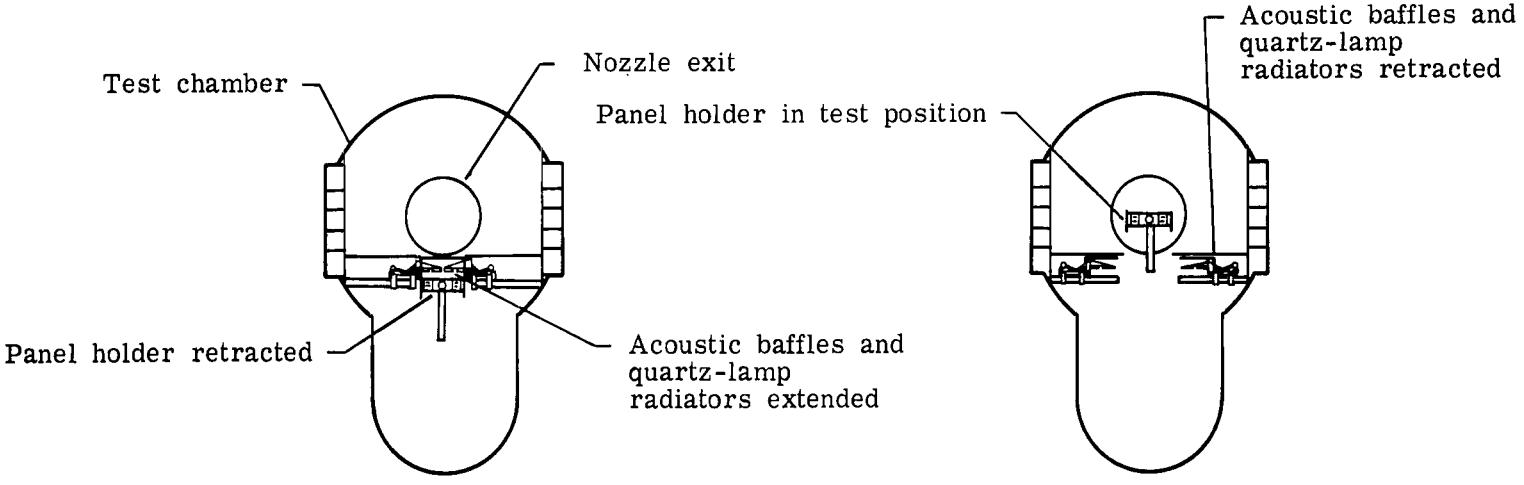

(b) Model position during preheat.

(c) Model position during test.

Figure 14.- Langley 8-foot high-temperature structures tunnel. Dimensions are in m (ft).

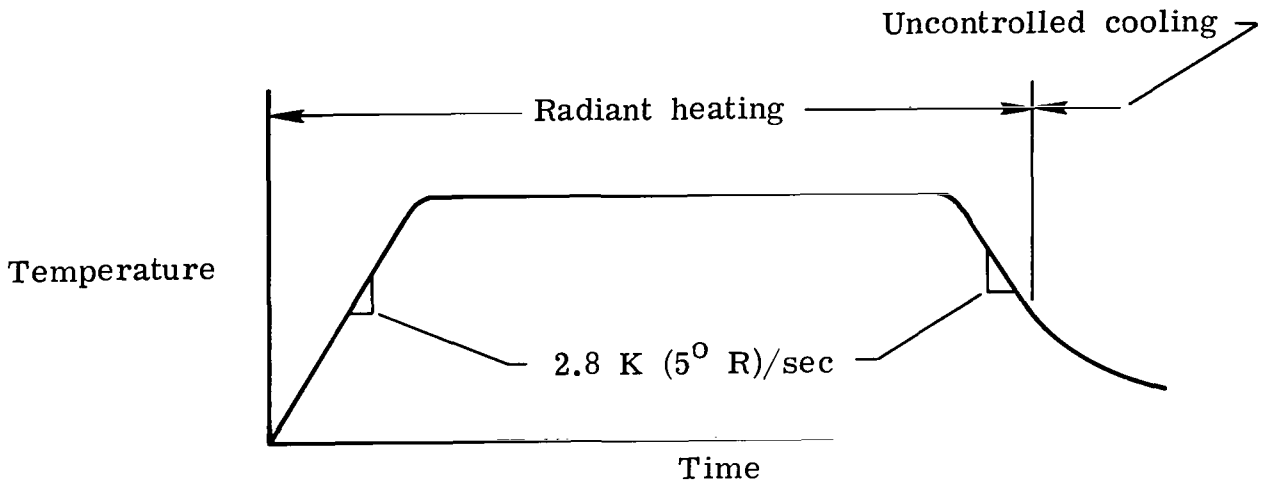

(a) Thermal cycle by radiant heating.

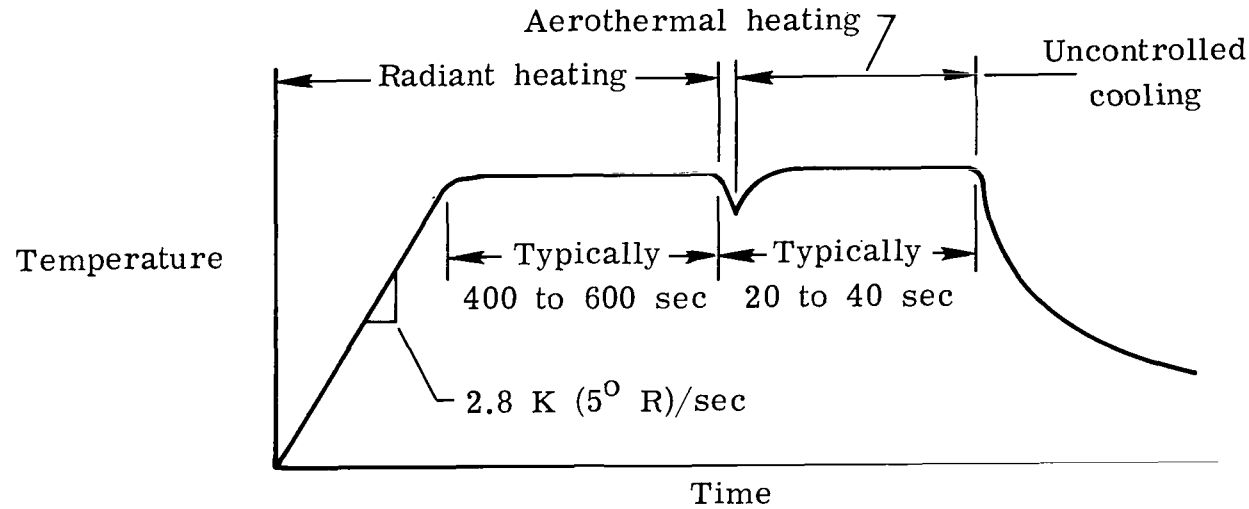

(b) Radiant-preheat—aerothermal exposure.

Figure 15.- Typical surface temperature time histories.

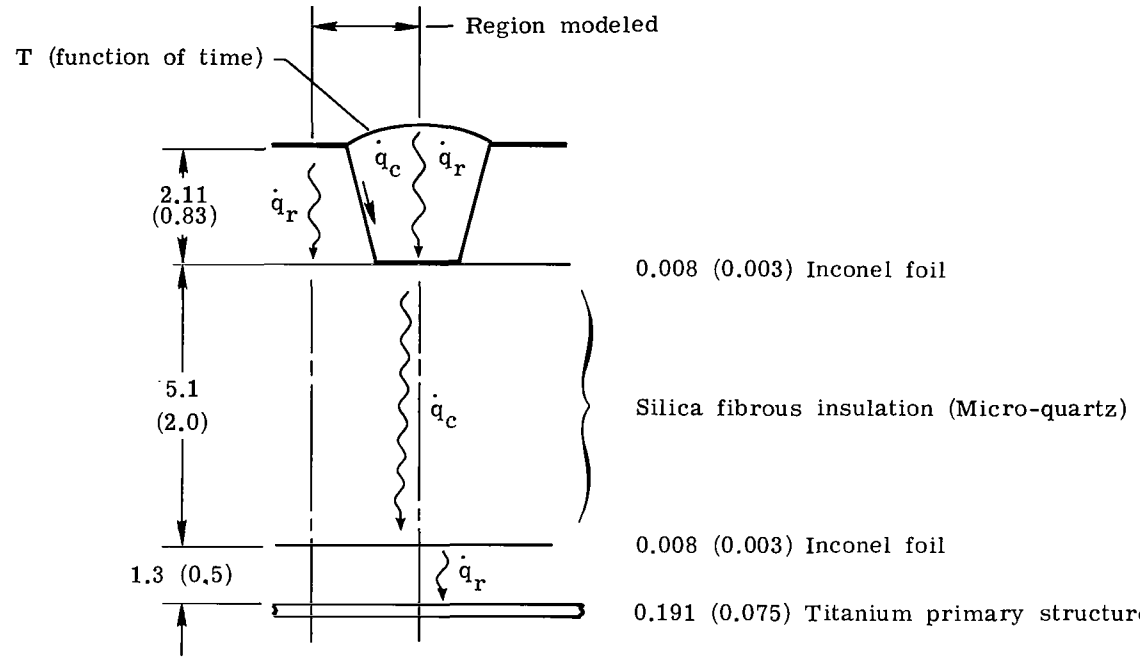

Figure 16.- Panel components and heating modes used in the thermal analysis. Dimensions are in cm (in.).

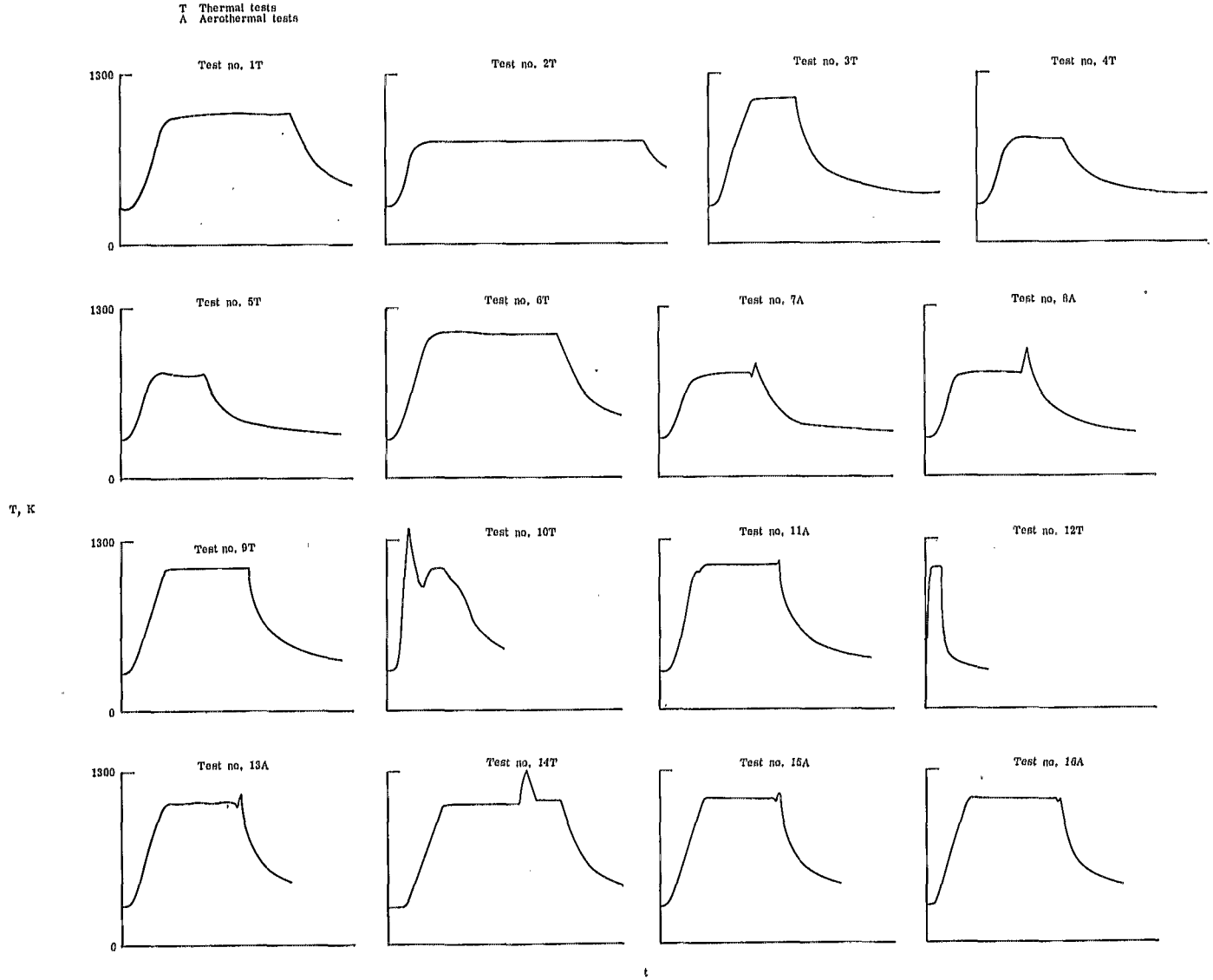

Figure 17.- Test panel surface temperature time histories.

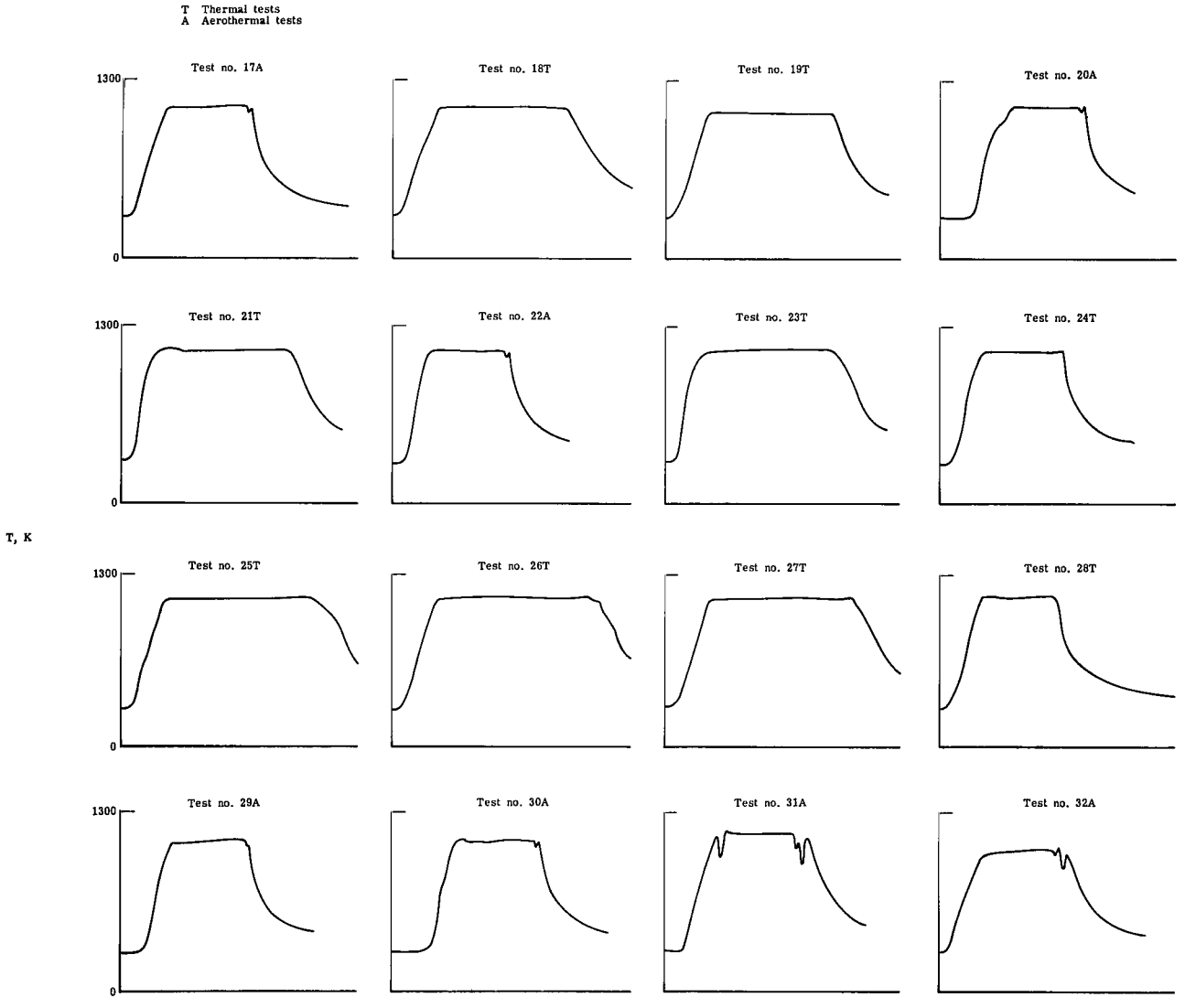

Figure 17.- Concluded.

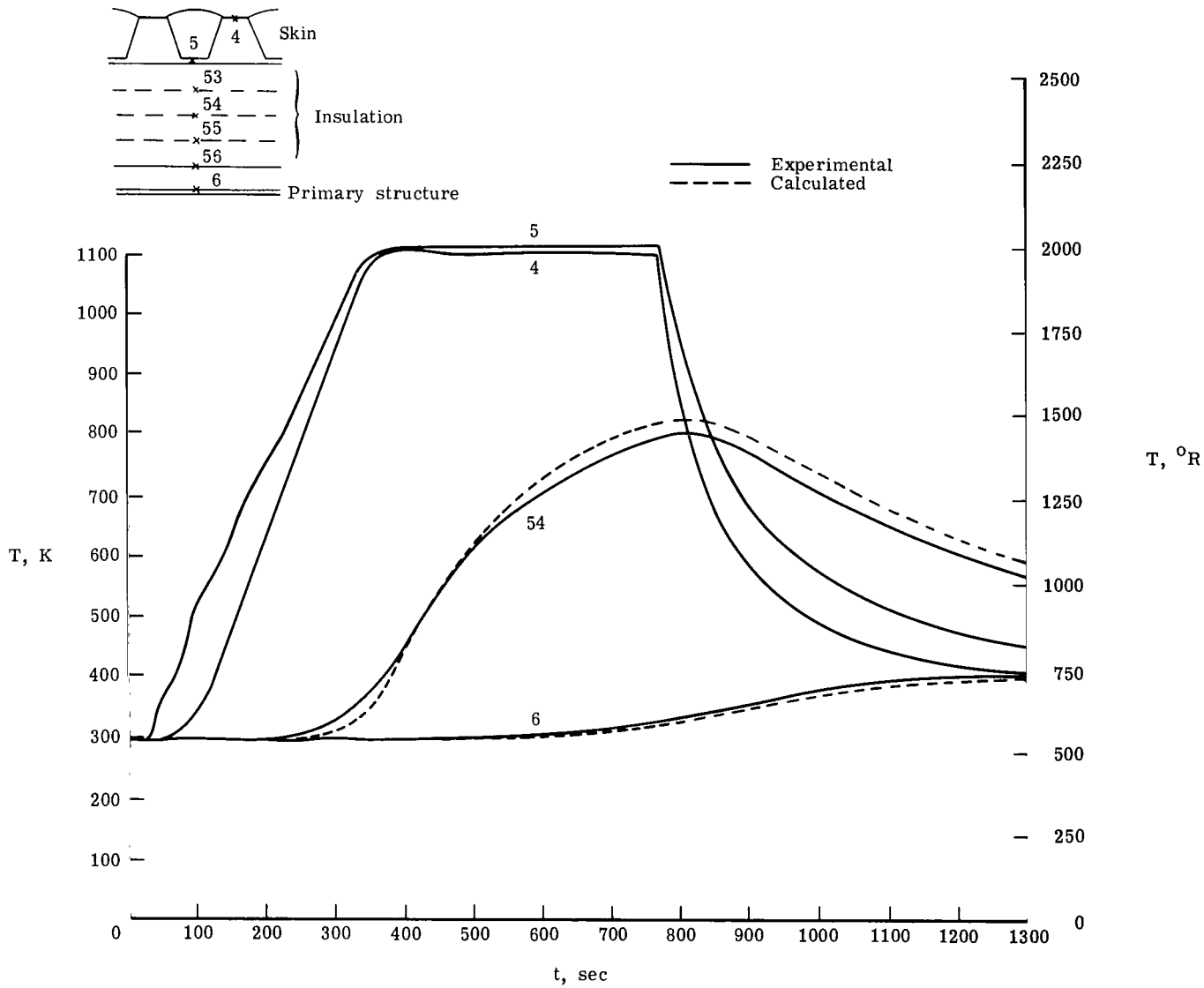

(a) Center of panel.

Figure 18.- Typical radiant-heating temperature time histories at various locations and depths through panel. (Test 3.)

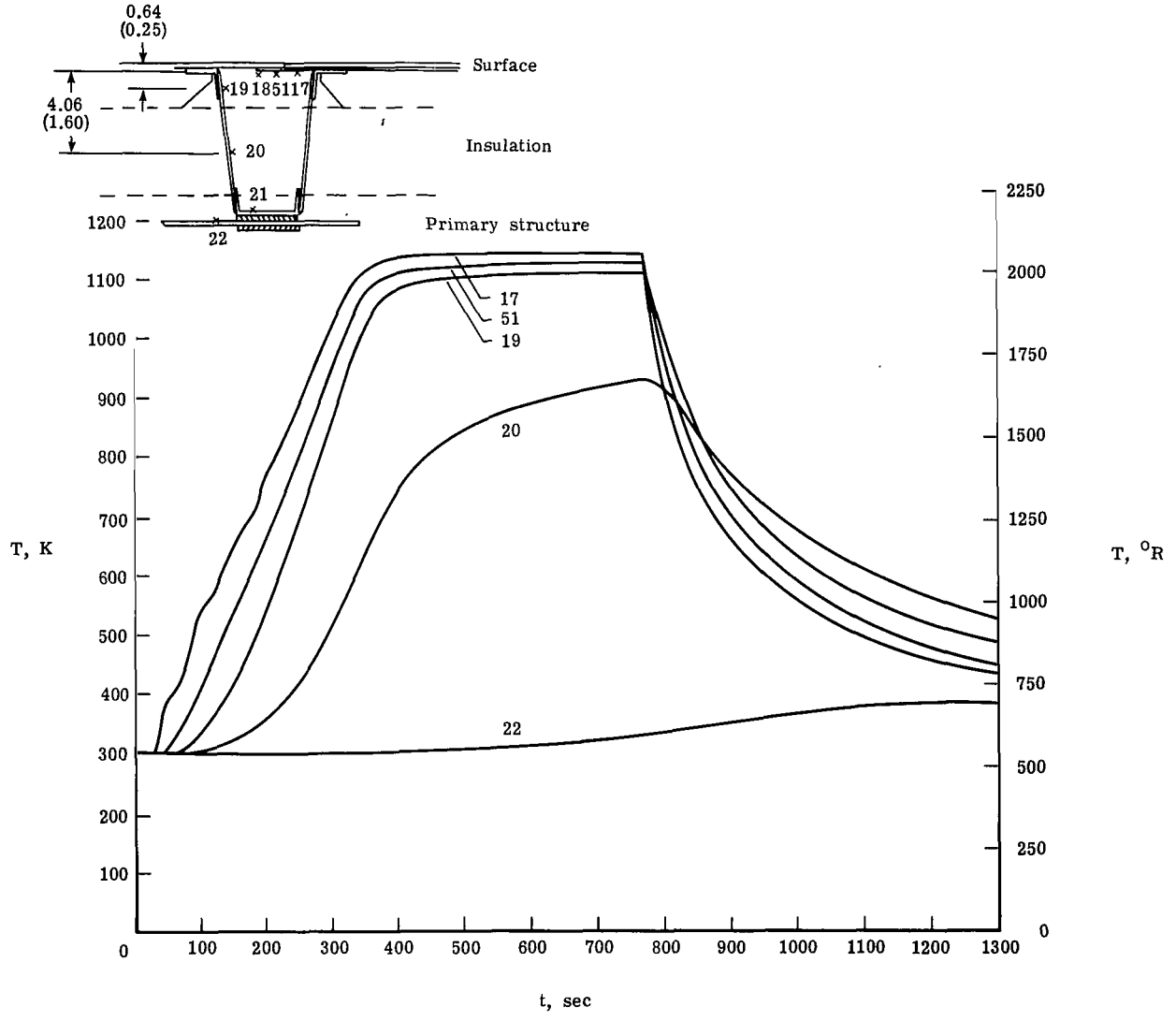

(b) Along shingle-slip joint and support.

Figure 18.- Continued.

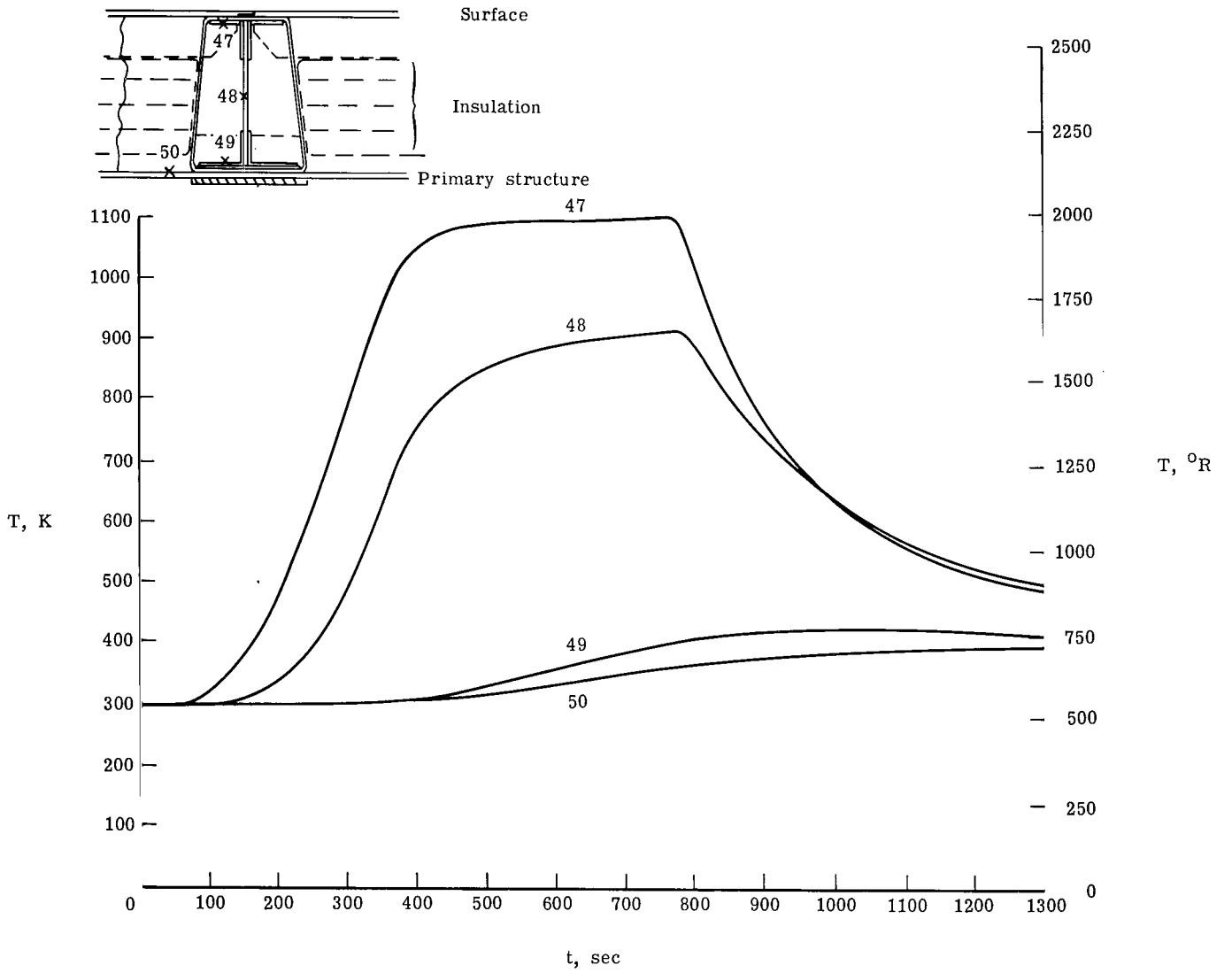

(c) Along drag support.

Figure 18.- Concluded.

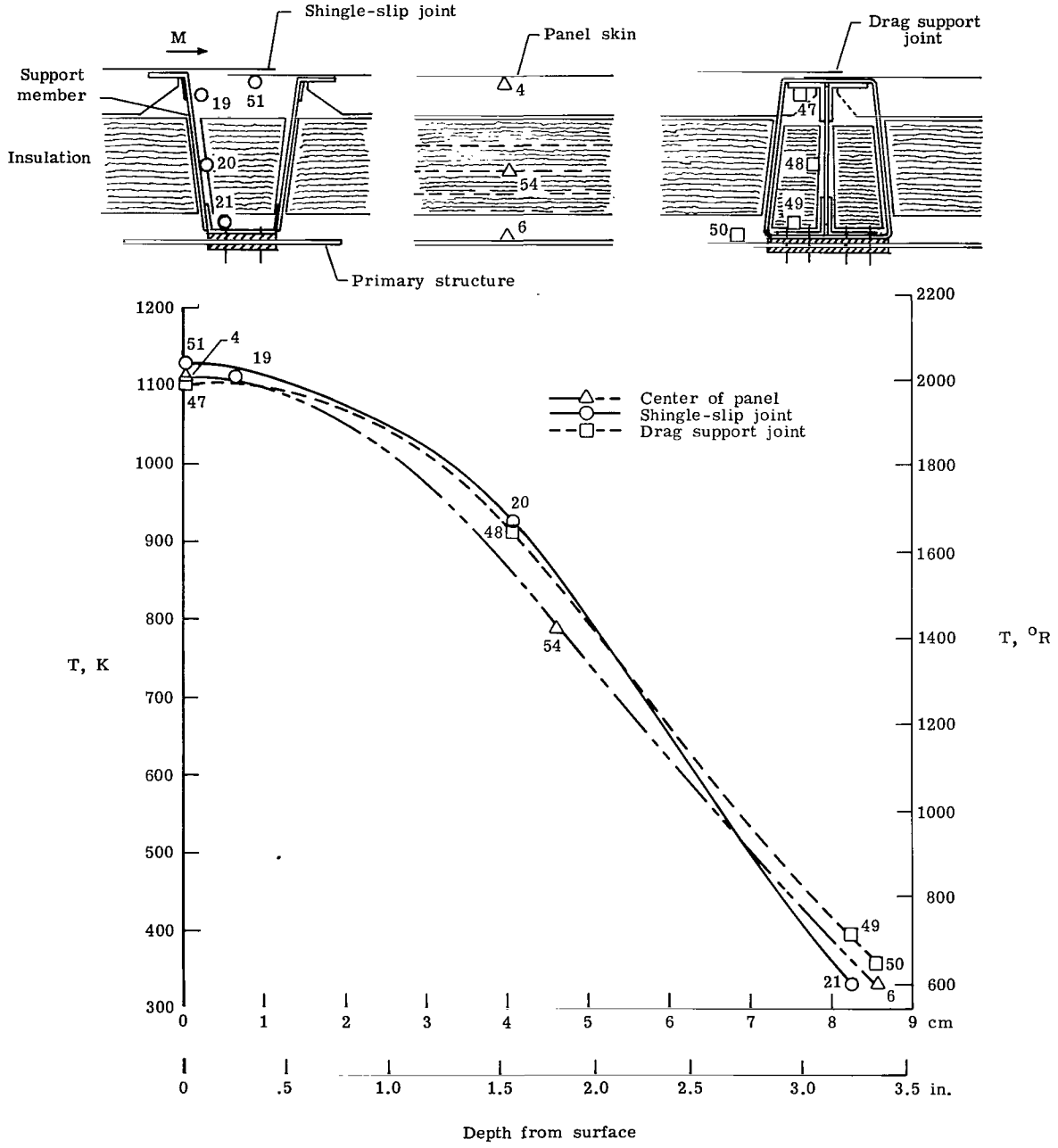

Figure 19.- Typical radiant-heating temperature distributions through depth of TPS after 750 sec. (Test 3.)

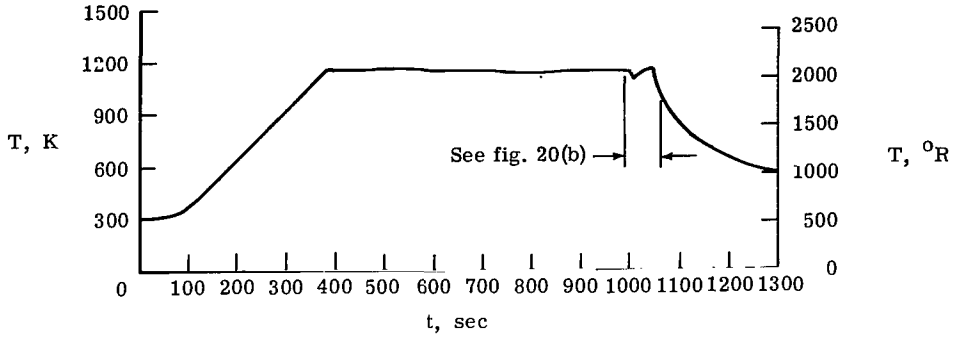

(a) Surface-temperature history.

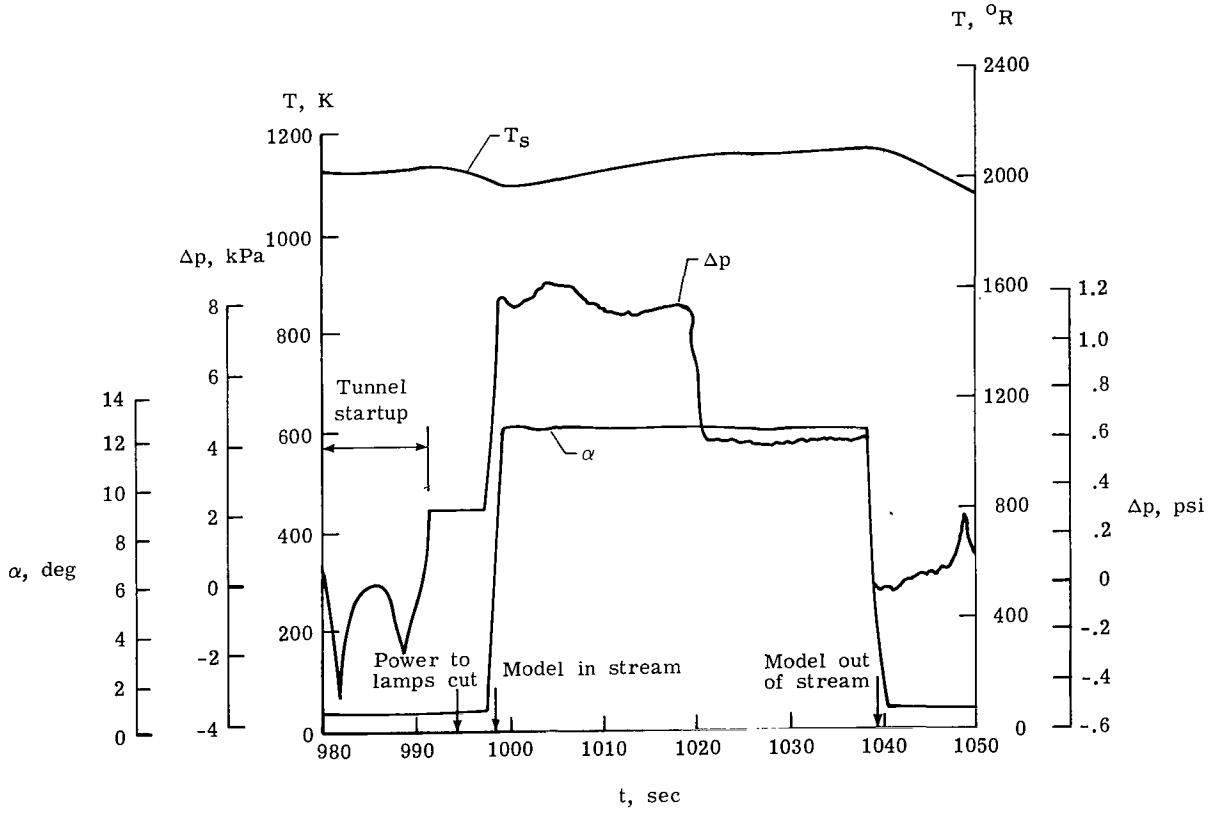

(b) Surface temperature, differential pressure, and angle of attack during aerothermal test.

Figure 20.- Environment imposed on TPS panel during test 15.

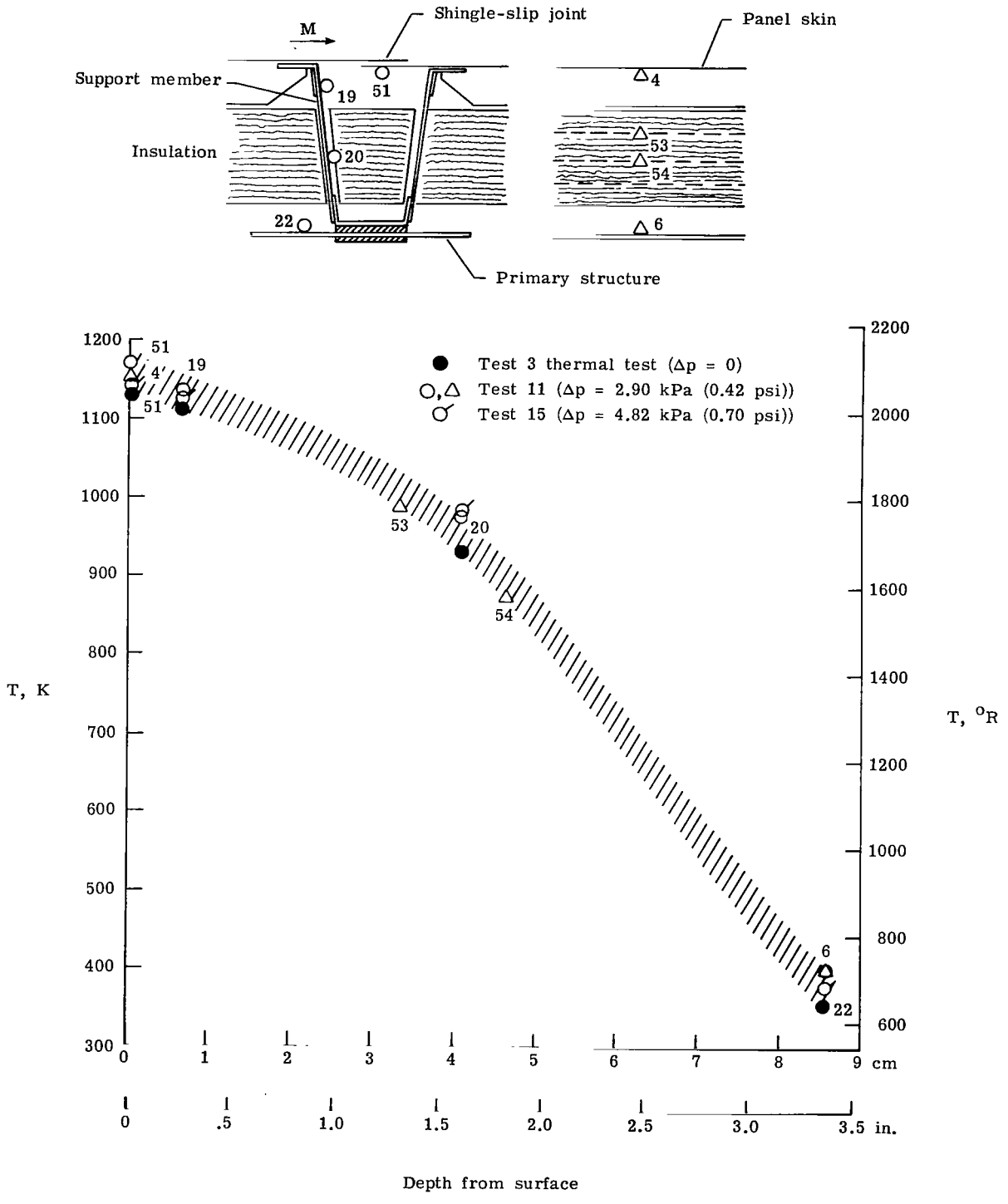

Figure 21.- Typical aerothermal temperature distributions through depth of panel.

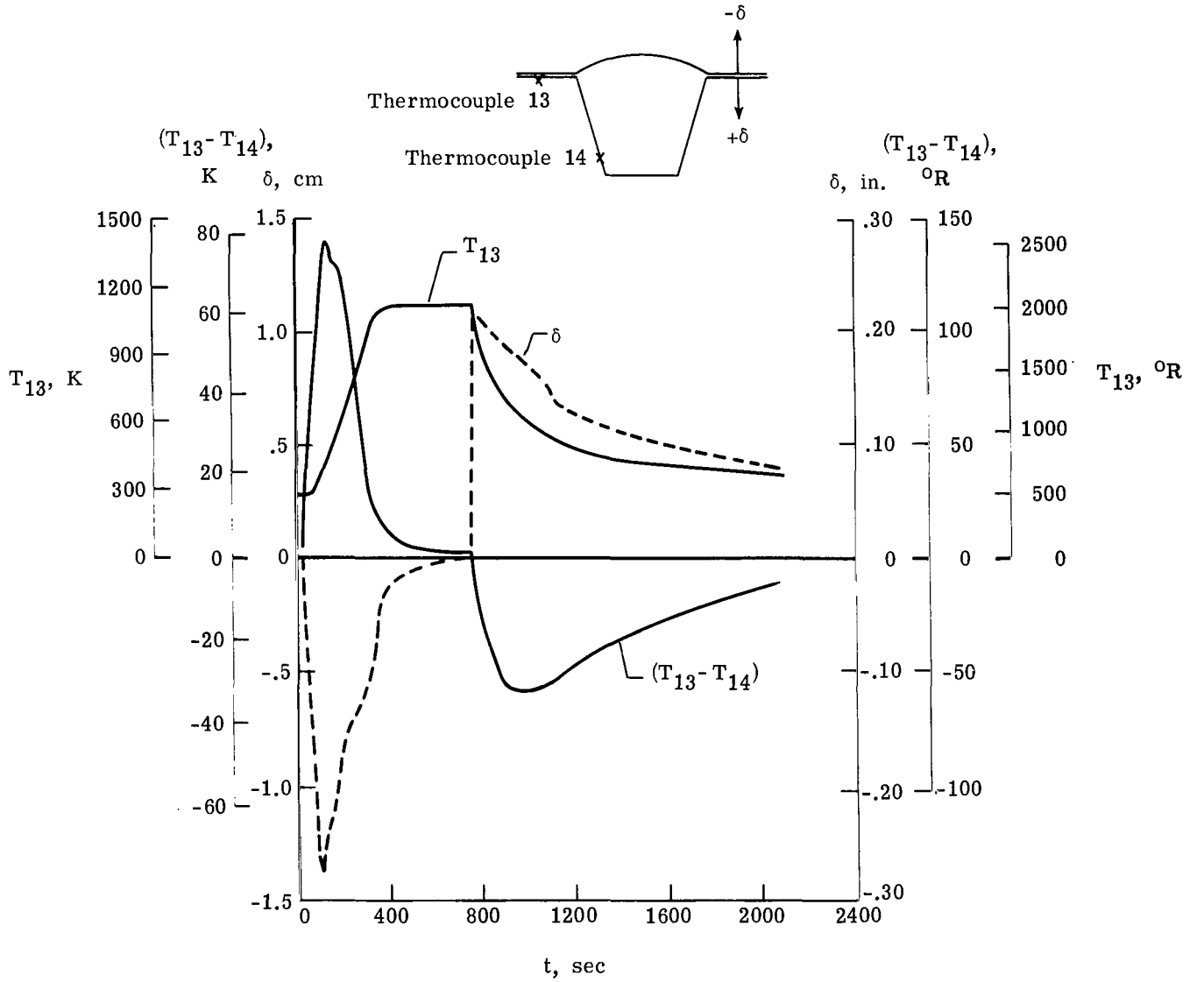

Figure 22.- Temperatures and deflections at center of panel during radiant heating for test 3.

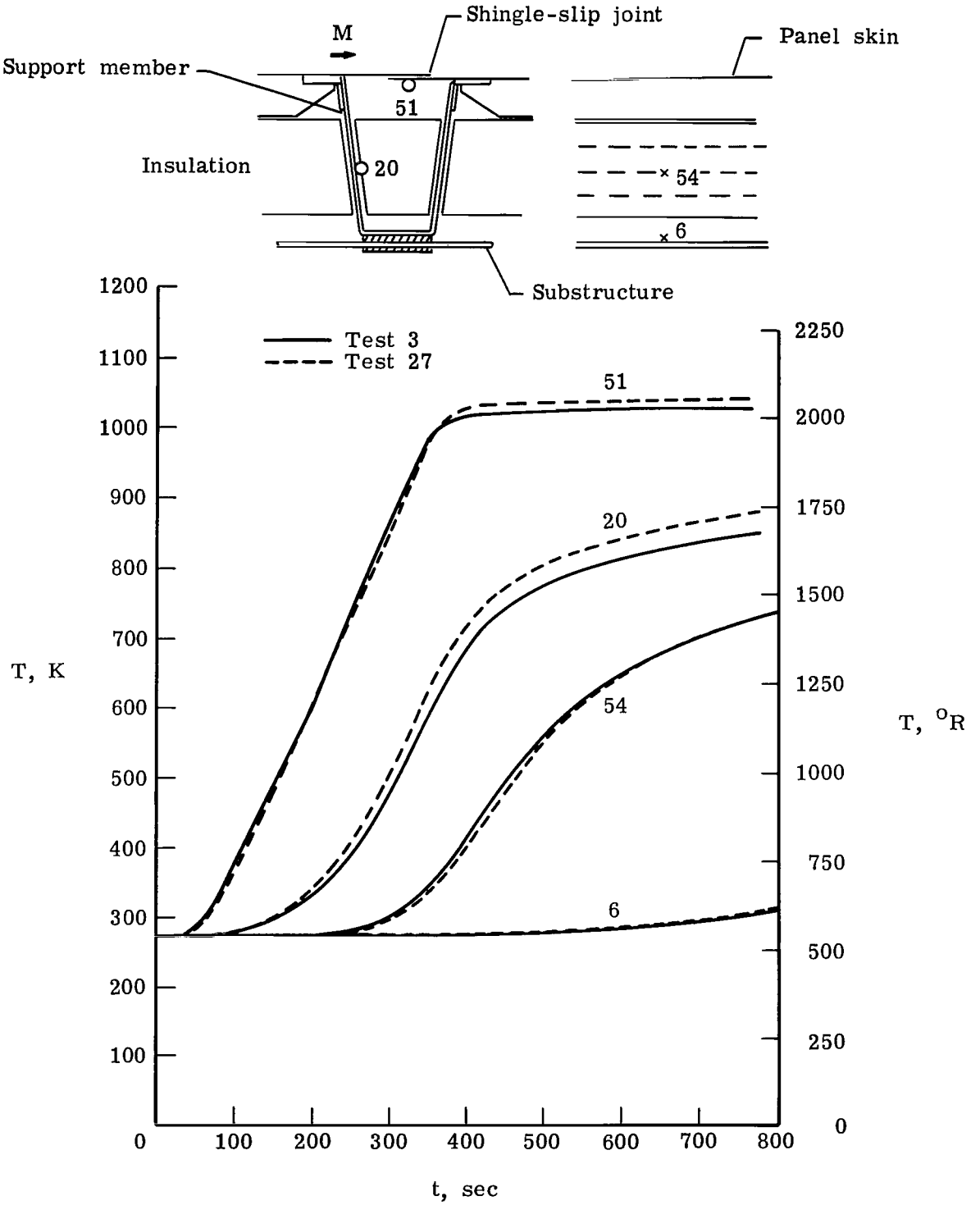

Figure 23.- Comparison of temperature time histories near beginning and end of test series.

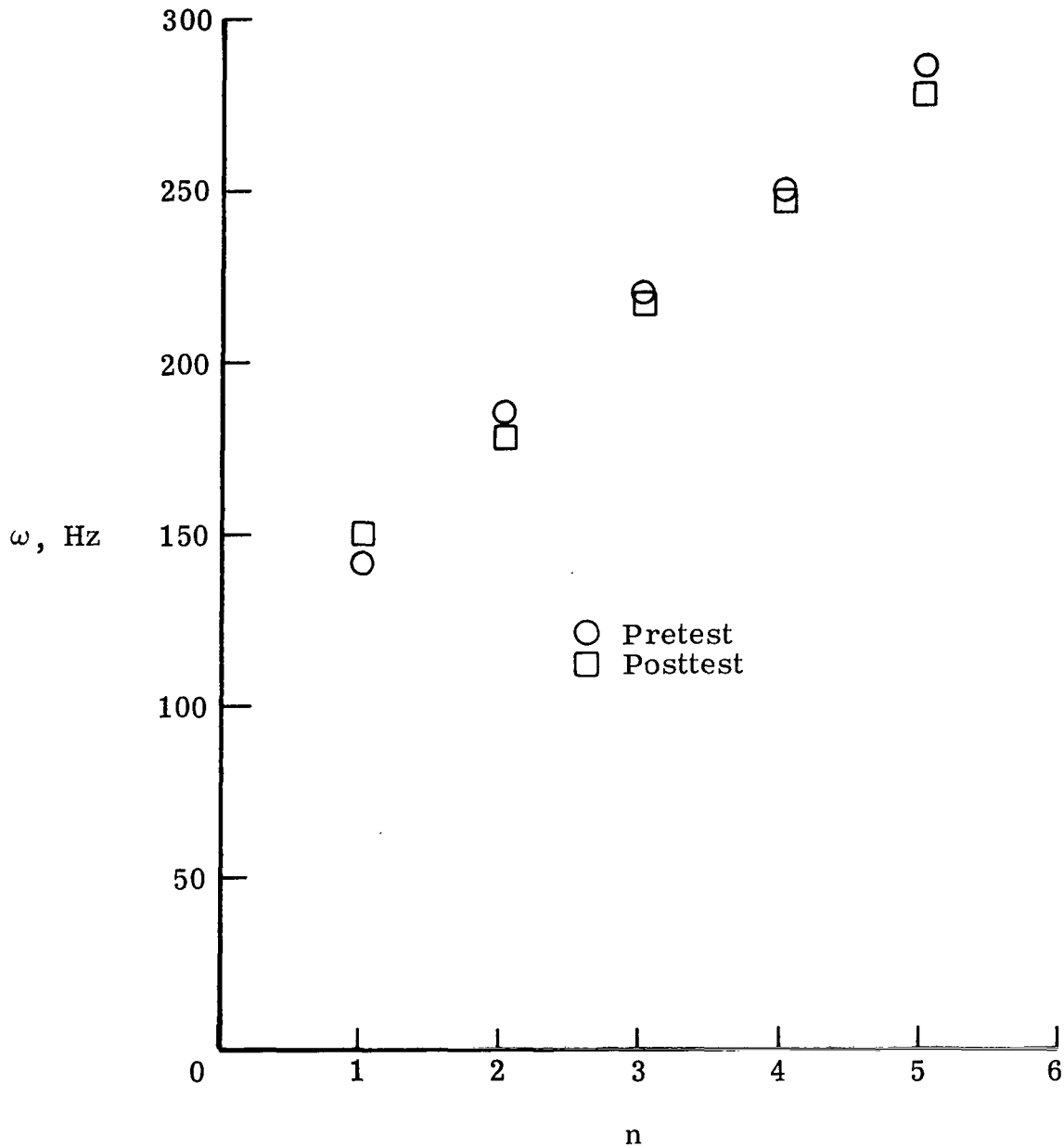

Figure 24.- Measured natural frequencies before and after the test series for one bay of the panel.

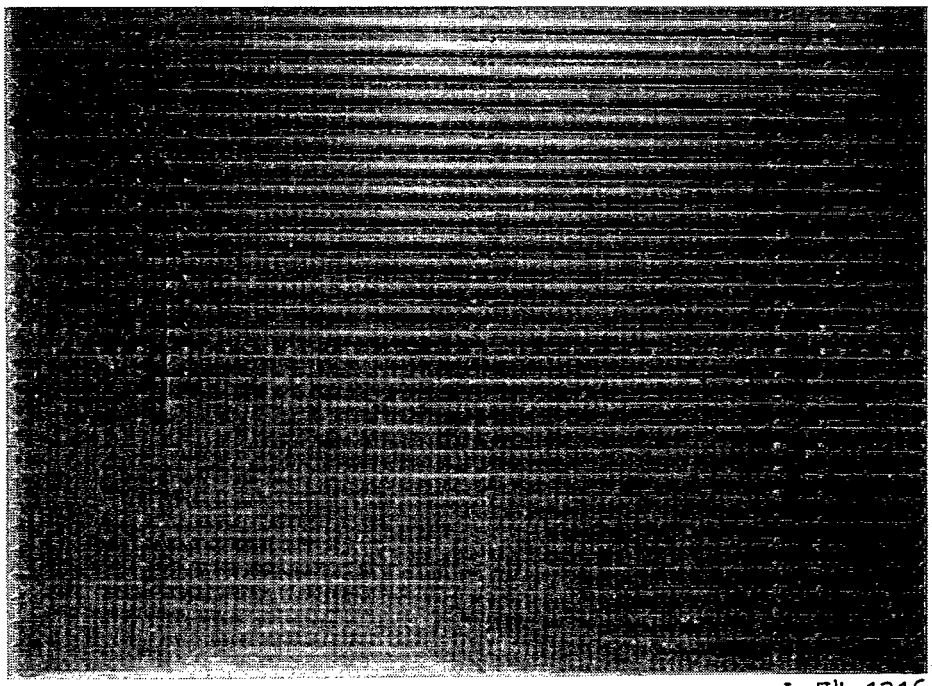

L-74-1316

(a) Before tests.

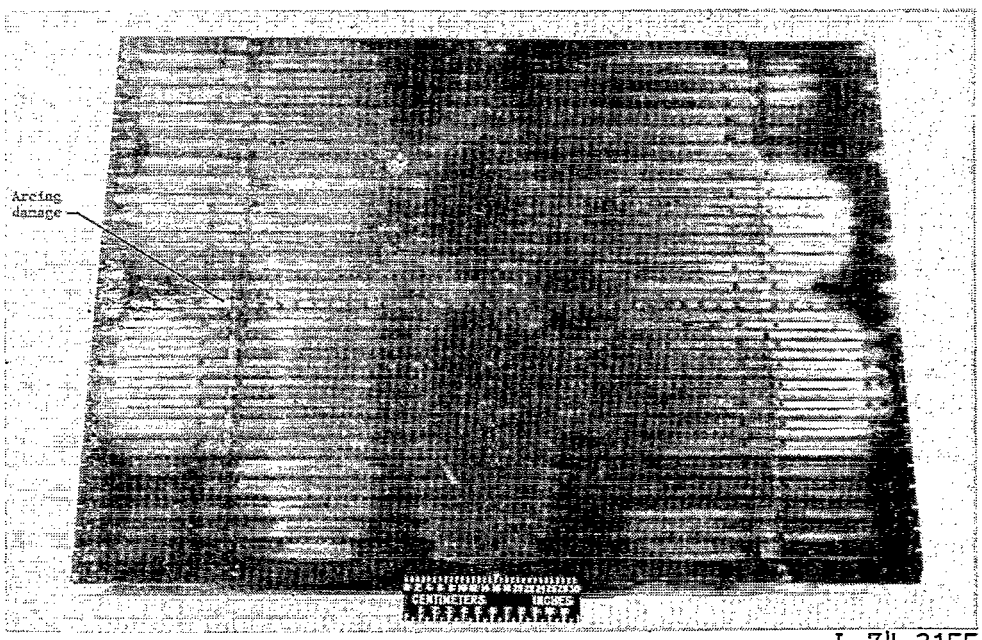

L-74-3155

(b) After tests.

Figure 25.- Panel before and after tests.

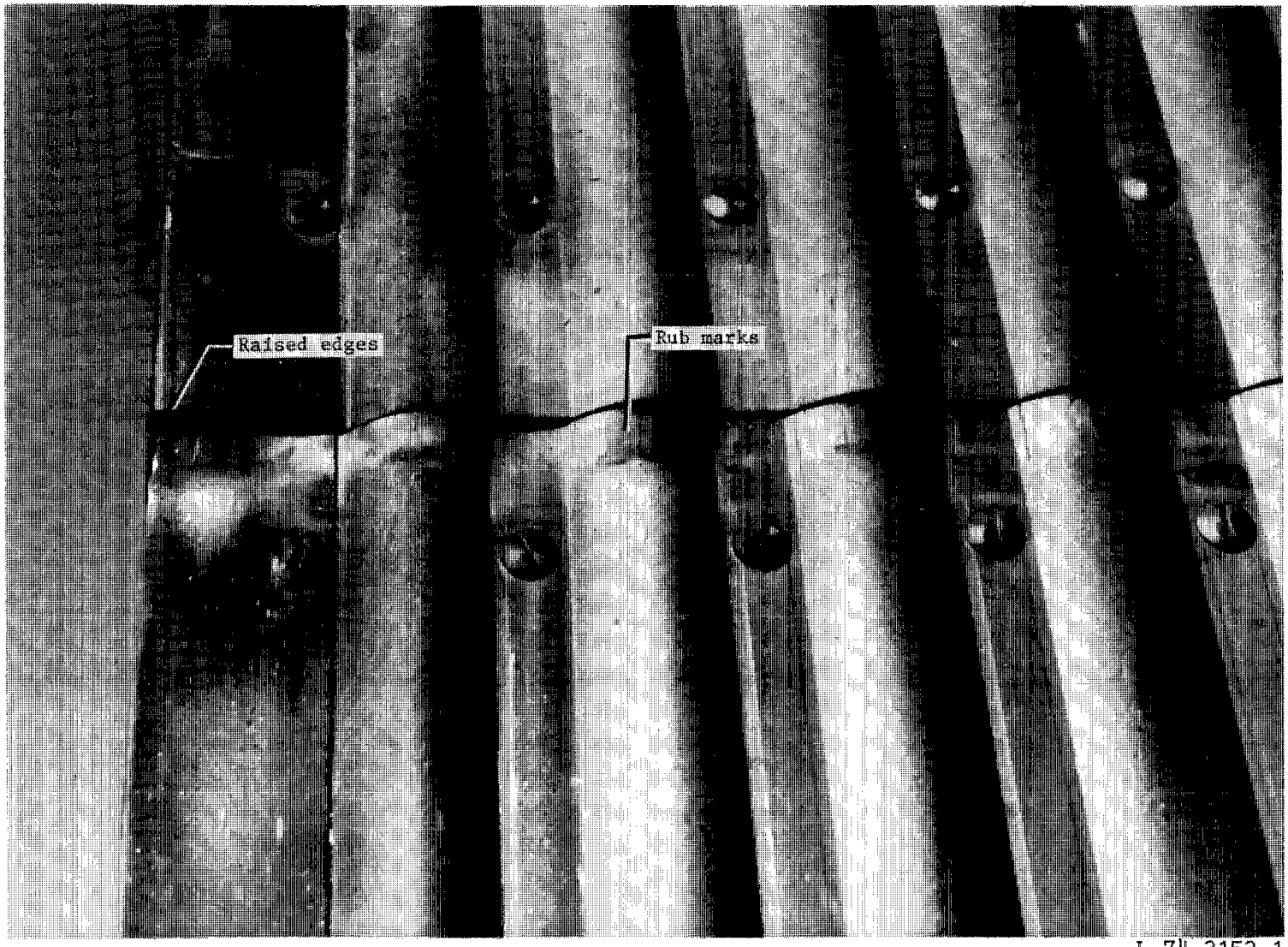

L-74-3153.1

Figure 26.- Shingle-slip joint near the side edge of the panel after tests.

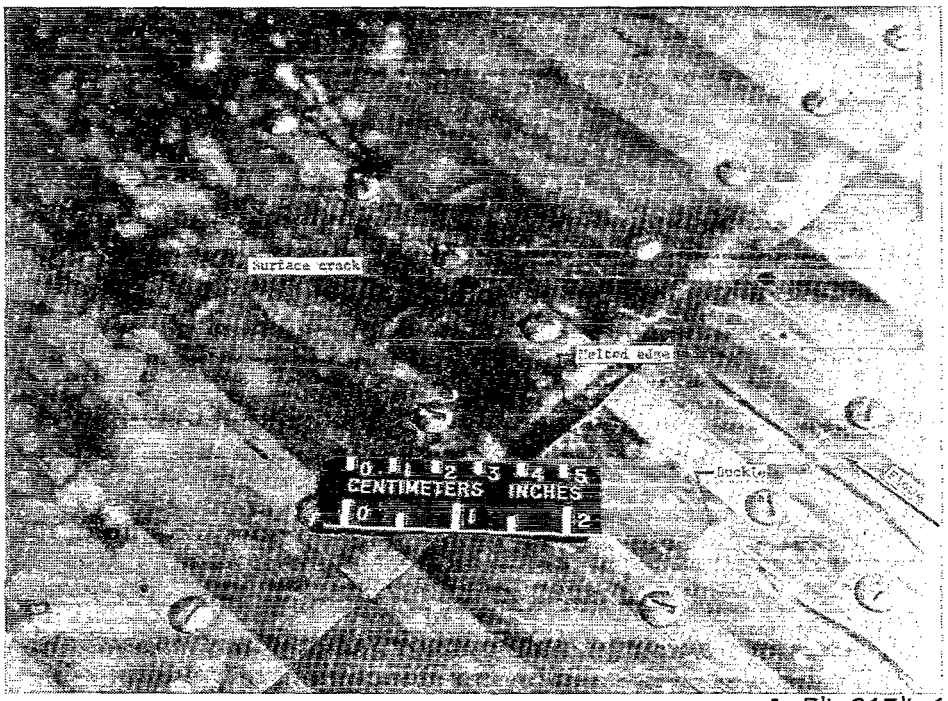

L-74-3154.1

(a) Damage due to arcing between lamps and panel.

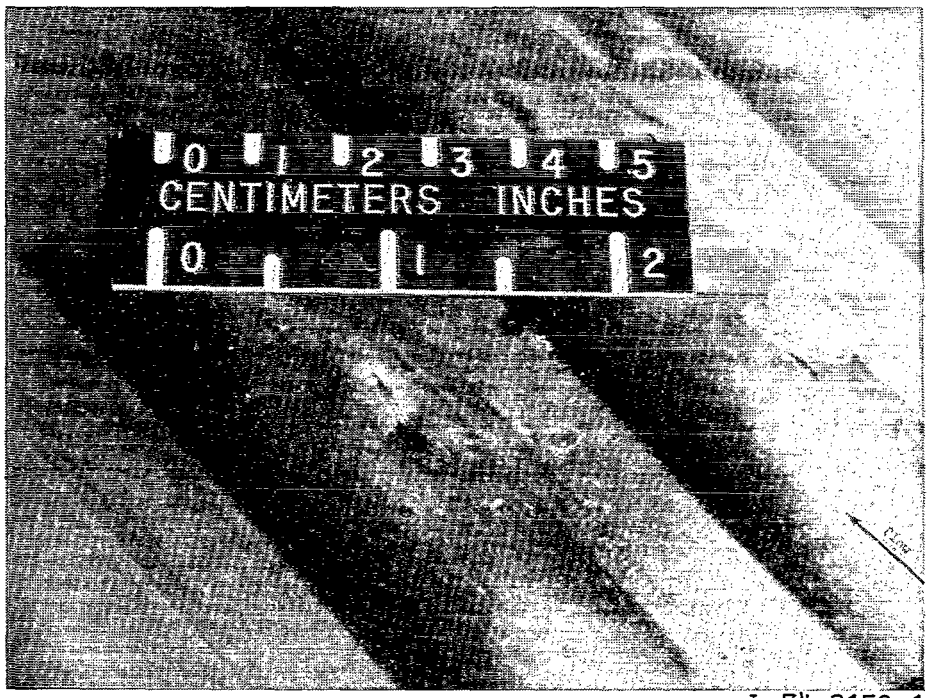

L-74-3159.1

(b) Particle-impact damage.

Figure 27.- Posttest panel surface damage.

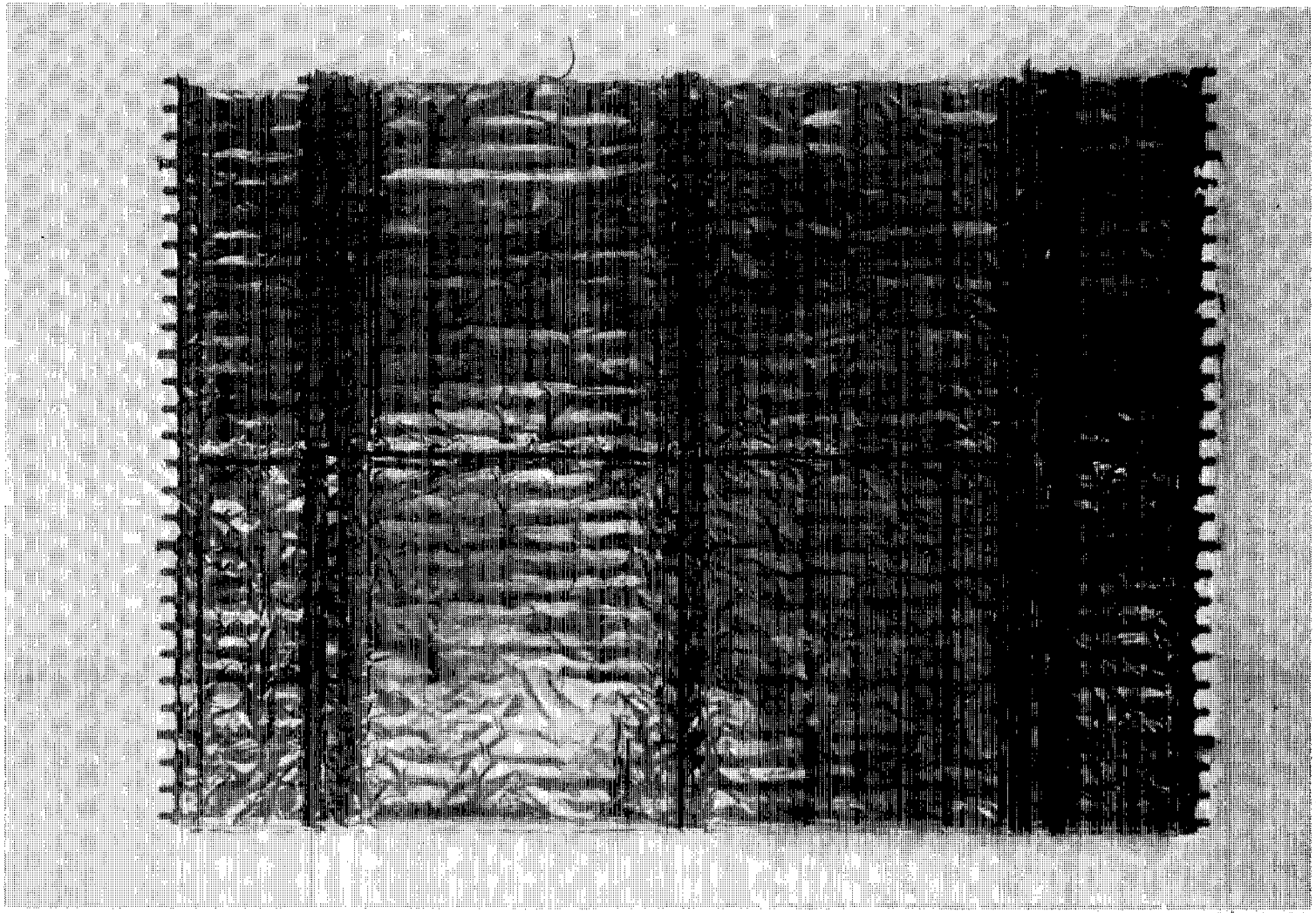

L-74-2109

Figure 28.- Posttest conditions of insulation package.

NASA-Langley, 1977 L-11286

NATIONAL AERONAUTICS AND SPACE ADMINISTRATION
WASHINGTON, D.C. 20546

OFFICIAL BUSINESS
PENALTY FOR PRIVATE USE $300

SPECIAL FOURTH-CLASS RATE
BOOK

POSTAGE AND FEES PAID
NATIONAL AERONAUTICS AND
SPACE ADMINISTRATION
451

U.S.MAIL

271 001 C1 U D 770408 S00903DS
DEPT OF THE AIR FORCE
AF WEAPONS LABORATORY
ATTN: TECHNICAL LIBRARY (SUL)
KIRTLAND AFB NM 87117

POSTMASTER: If Undeliverable (Section 158 Postal Manual) Do Not Return

"The aeronautical and space activities of the United States shall be conducted so as to contribute . . . to the expansion of human knowledge of phenomena in the atmosphere and space. The Administration shall provide for the widest practicable and appropriate dissemination of information concerning its activities and the results thereof."

—NATIONAL AERONAUTICS AND SPACE ACT OF 1958

NASA SCIENTIFIC AND TECHNICAL PUBLICATIONS

TECHNICAL REPORTS: Scientific and technical information considered important, complete, and a lasting contribution to existing knowledge.

TECHNICAL NOTES: Information less broad in scope but nevertheless of importance as a contribution to existing knowledge.

TECHNICAL MEMORANDUMS: Information receiving limited distribution because of preliminary data, security classification, or other reasons. Also includes conference proceedings with either limited or unlimited distribution.

CONTRACTOR REPORTS: Scientific and technical information generated under a NASA contract or grant and considered an important contribution to existing knowledge.

TECHNICAL TRANSLATIONS: Information published in a foreign language considered to merit NASA distribution in English.

SPECIAL PUBLICATIONS: Information derived from or of value to NASA activities. Publications include final reports of major projects, monographs, data compilations, handbooks, sourcebooks, and special bibliographies.

TECHNOLOGY UTILIZATION PUBLICATIONS: Information on technology used by NASA that may be of particular interest in commercial and other non-aerospace applications. Publications include Tech Briefs, Technology Utilization Reports and Technology Surveys.

Details on the availability of these publications may be obtained from:

SCIENTIFIC AND TECHNICAL INFORMATION OFFICE

NATIONAL AERONAUTICS AND SPACE ADMINISTRATION

Washington, D.C. 20546